Threshold pion photo-production off nucleons using the nuclear model with explicit pions

Martin Mikkelsen
201706771

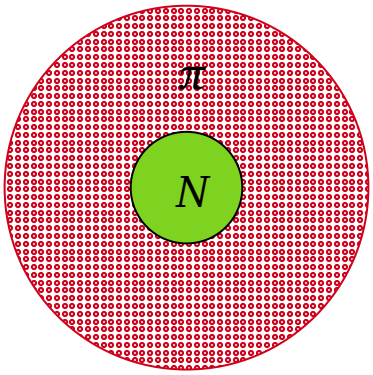

Master's thesis
Supervisor: Dmitri Fedorov

Department of Physics and Astronomy
Aarhus University
Denmark

November 2022

Summary

This is a bachelor's project about relativistic kinematics. This means a theoretical description of particle's motion without considering the forces that cause them to move, in the relativistic limit. More specifically this project illuminates three-particle decays with kinematic invariant quantities. The theory introduces an approach to examine an anomaly that occurred in an experiment when a Hungarian research team measured transitions in ^{8}Be. It combines considerations of phase space for three-particle decay with resonance amplitudes and angular distributions. This leads to experimental predictions separated into three parts depending on the spin state of the resonant particle, the X17 particle. This project concludes that the formalism is consistent with the relativistic scattering angles in the laboratory system and how experimental results can be illustrated using kinematic invariants. Three angles are proposed to investigate the X17 particle experimentally.

Resumé

Dette bachelorprojekt omhandler relativistisk kinematisk. Det vil altså sige en teoretisk beskrivelse af partiklers bevægelse uden ydre påvirkning i den relativistiske grænse. Mere specifikt belyser dette projekt 3-partikel henfald ved hjælp af kinematiske invariante størrelser. Teorien i projektet introducerer den tilgang, der er anvendt til at undersøge en anormalitet i et forsøg, som opstod da et ungarnsk forskerhold målte overgange i ^{8}Be. Teorien kombinerer overvejelser omkring faserum for tre-partikel henfald med resonansamplituder og vinkelfordelinger. Dette fører til eksperimentelle forudsigelser, der er inddelt i tre dele afhængig af spintilstanden for resonanspartiklen, X17. Projektet konkluderer, at formalismen er konsistent med den relativistiske spredningsvinkel i laboratoriets hvileramme og viser hvordan eksperimentelle resultater kan repræsenteres ved kinematiske invariante størrelser. Der foreslås tre vinkler, som kan måles eksperimentelt for at undersøge X17 partiklen.

Colophon

Threshold pion photo-production off nucleons using the nuclear model with explicit pions

Master's thesis by Martin Mikkelsen

The project is supervised by Dmitri Fedorov

Typeset by the author using LaTeX and the memoir document class. Figures are made with the using the Seaborn package in Python and the Tikz package.

Code for document, figures and numerical calculations can be found on `https://github.com/MartinMikkelsen`

Printed at Aarhus University

Contents

Chapter 1

Introduction

Nuclear physics covers and expands different ideas from other areas of physics. These include but are not limited to low- and high-energy physics, few- and many-body dynamics, and classical and quantum statistical mechanics. Two concepts are needed when discussing nuclear physics: the nucleon and mesons. Protons and neutrons have very similar properties, and the unifying term nucleon refers to a mass of around 1 GeV. Nuclei consist of nucleons and are held together by the nuclear forces–by exchanging mediating quanta called mesons. This is similar to how the photon exchange generates the electromagnetic force. There are many different mesons, but the lightest mesons are called the pions (π^-, π^0, π^+) with a mass of about one-seventh of the nucleon leaving us in the MeV range. This energy scale also defines the regime known as low-energy physics, where the nucleus can be considered non-relativistic, and the mesons are virtual particles hidden in nucleon-nucleon interactions. Generally speaking, within the domain of low-energy nuclear physics, the nucleus appears as a self-bound many-body nucleonic system with intrinsic degrees of freedom. These systems are mesoscopic, along with atoms, molecules, micro- and nano-devices of condensed matter systems, and quantum computers. This means they are sufficiently large to have statistical regularities yet also small enough to study individual quantum states.

Increasing the energy will reveal the intermediate region of nuclear physics. Here relativistic effects become more important, and the meson and nucleon excitations become explicit. This energy scale is loosely characterized by an energy scale of a few GeV. At even higher energies and higher momentum transfer, dissecting the constituent of the nucleons and mesons is possible. These are known as quarks and gluons, and now the energy scale is in the TeV range. Generally speaking, the field of nuclear physics covers an energy range from KeV to TeV and the two different regimes of relativistic effects.

1.1 Strong interactions

Using the uncertainty relation one can estimate the range of the nuclear forces. If we assume the interaction is mediated by a quanta being emitted by one particle and absorbed by another particle we gain insight into two properties of the strong nuclear force. Firstly, how the pion exchange as a mechanicsm for the nucleon interaction and how the range of the strong nuclear force is charachterized by the Compton wavelength of the lightest possible mediator. In the case of the neutral pion is this approximately 1.46 fm.

1.2 Outline of Thesis

This thesis is organised as follows. We will introduce the model in chapter 3. We will go through how the nuclear model with explicit mesons will be constructed generally. Then we consider the case where the mesons are pions and look at how we can determine an equation of motion for the pion-nucleon system. We then focus specifically on the one-pion approximation, which is the most straightforward appearance of the nuclear model with explicit pions off protons. This is closely related to how we formulate the dressing of the proton and arrive at an equation of motion that is to be solved. This is the subject of section 3.4 where we explore the flexibility of this model. Specifically, this means we test different form factors and do a relativistic expansion to explore how this affects the solutions found in the previous section. Finally, we test how changing the operator to an operator found in effective field theory affects the system. In section 4 we explore pion photoproduction using the model with explicit pions and how this emerges naturally as a photodisintegration process. We consider the four possible reactions: two off the proton and two off the neutron. To calculate the matrix elements, we make a dipole approximation in section 4.1, and an exact approach follows this in section 4.2. We do fits to extract the parameters for the model and compare to experimental data.

Chapter 2

Theoretical background

2.1 Interaction of Radiation with Matter

In the following, we will derive the necessary equations describing how a quantized field interacts with matter within the framework of the second quantization. We will assume the final quantized form of the vector potential given by

$$\mathbf{A}(\mathbf{r},t)=\sum_{\mathbf{k},\lambda}\sqrt{\frac{2\pi\hbar c^2}{\omega_k V}}\left(a_{k,\lambda}\mathbf{e}_{\mathbf{k},\lambda}\mathrm{e}^{i(\mathbf{k}\cdot\mathbf{r})-i\omega_k t}+a^{\dagger}_{\mathbf{k},\boldsymbol{\lambda}}\mathbf{e}^{*}_{\mathbf{k},\lambda}\mathrm{e}^{-i(\mathbf{k}\cdot\mathbf{r})+i\omega_k t}\right) \quad (2.1)$$

We now consider a non-relativistic system of charged particles interacting with the electromagnetic field. In this thesis, we will consider a two-particle system, but in this section, we generalize the results to any integer of particles denoted by the subscript i. The interaction will enable the system to emit and absorb photons. We start with the usual Hamiltonian describing the many-body system given by $H_0(\mathbf{r}_i),\mathbf{p_i}$ with no field. We introduce a field and do the following substitution

$$\mathbf{p}_i\rightarrow\mathbf{p}_i-\frac{e_i}{c}\mathbf{A}(\mathbf{r}_i), \quad (2.2)$$

where e_i is the charge of the i'th particle and c is the speed of light. This leads to a new Hamiltonian, which now depends on the field variables

$$H_0\rightarrow H_0'=H_0\left(\mathbf{r}_i,\mathbf{p}_i-\frac{e_i}{c}\mathbf{A}(\mathbf{r}_i)\right)+\sum_i e_i\phi(\mathbf{r}_i), \quad (2.3)$$

where the last term in equation (2.3) is the potential energy. We now introduce the radiation gauge choice, which is purely conventional and any other choice of gauge will result in the same equations, albeit more difficult. The radiation gauge is given by

$$\boldsymbol{\nabla}\cdot\mathbf{A}=\phi=0, \quad (2.4)$$

and the non-relativistic Hamiltonian of the system describing the interaction with the radiation field is given by

$$H=\sum_i\frac{1}{2m_i}\left(\mathbf{p}-\frac{e_i}{c}\mathbf{A}(\mathbf{r}_i)\right)^2, \quad (2.5)$$

where $\mathbf{A}(\mathbf{r}_i)$ is equation (2.1) at point $\mathbf{r}_i$. We assumed the interaction between particles depends on their coordinate, so the minimal inclusion of the electromagnetic field affects only the kinetic part. This is a

1. One could add a spin-orbit term to the non-relativistic approach, but this is not necessary for our calculations later

fair approximation in the non-relativistic limit and does not account for velocity-dependant interactions such as spin-orbit[1]. The electromagnetic interaction is relatively weak, and its strength is given by the fine structure constant, $\alpha = e^2/(\hbar c)$. Generally speaking, this interaction can be taken into account in the lowest non-vanishing order of perturbation theory. We expand (2.5) and keep only the linear terms

$$H^{(1)} = -\sum_i \frac{e_i}{2m_i c}(\mathbf{p}_i \cdot \mathbf{A}(\mathbf{r}_i) + \mathbf{A}(\mathbf{r}_i) \cdot \mathbf{p}_i), \tag{2.6}$$

where the (1) represents the first non-vanishing order. Due to our choice of gauge equation (2.4) the two terms in (2.6) commute and we are left with

$$H = -\sum_i \frac{e_i}{m_i c}\mathbf{A}(\mathbf{r}, t)\mathbf{p}. \tag{2.7}$$

For the type of problems we will be solving in 4 we will be working mainly with one charged particle, and we can ignore the sum in (2.7).

2.2 Density of states

As mentioned in section 2.1 the electromagnetic interaction strength is related to the fine structure constant. In section 4 we want to do perturbation theory to get an expression for the total cross-section as a function of energy which the relatively weak fine structure constant allows. From perturbation theory, the transition rate is described by Fermi's golden rule given by

$$\mathrm{d}\omega = \frac{2\pi}{\hbar}|\mathcal{M}|^2 \,\mathrm{d}\rho, \tag{2.8}$$

where the matrix element $\mathcal{M}$ is the subject in section 4 and $\mathrm{d}\rho$ is the density of states in the final states. In this section, we will derive general results of the density of states in a non-relativistic and relativistic limit. The density of states is defined by

$$\rho(E) = \frac{\mathrm{d}n(E)}{\mathrm{d}E}, \tag{2.9}$$

where $n(E)$ is the number of states with energy E. Consider the number of states within the momentum space volume

$$\mathrm{d}^3\mathbf{p} = p^2 \mathrm{d}p \,\mathrm{d}\Omega_q, \tag{2.10}$$

where the subscript q is used to empathize momentum space. We will use this notation throughout the thesis. Equation (2.10) corresponds to the momenta with magnitude from p to $p + \mathrm{d}p$ and within a cone of solid angle $\mathrm{d}\Omega_q$. This is illustrated on figure 2.1. We use the solutions to the Schrödinger equation for a particle confined in a large volume with periodic boundary conditions are travelling waves. This leads to the following expression

$$\rho(p)\,\mathrm{d}\rho = \left(\frac{L}{2\pi\hbar}\right)^3 \mathrm{d}^3\mathbf{p} = \frac{V}{(2\pi\hbar)^3} p^2 \,\mathrm{d}p \,\mathrm{d}\Omega_q. \tag{2.11}$$

In section 4 we are interested in the number of possible final states with energy in the range between E_f and $E_f + \mathrm{d}E_f$ so we express (2.11) in terms of energy. This is given by

$$\rho(E_f) = \frac{V p_f^2}{(2\pi\hbar)^3}\frac{\mathrm{d}p_f}{\mathrm{d}E_f}\,\mathrm{d}\Omega_q. \tag{2.12}$$

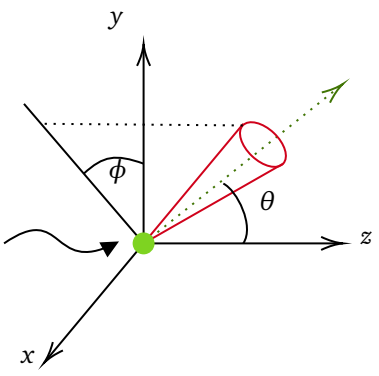

Figure 2.1: Differential cross section and the solid angle Ω_q (red cone).

This is the final expression non-relativistically. However, we want to generalize this result to also account for relativistic effects since we do not know what relativistic regime will dominate the process. For a general pion photoproduction process, we can write

$$N + \gamma \rightarrow N + \pi, \tag{2.13}$$

where N is the nucleon. The final state energy is then given by

$$E_f = E_N + E_\pi = \sqrt{p_f^2 c^2 + m_N^2 c^4} + \sqrt{p_f^2 c^2 + m_\pi^2 c^4}. \tag{2.14}$$

We now change the notation to match the variables used later in section 4 and write the final state momentum p_f in terms of the wave number q.

From conservation of energy, we get the following expression for the energy of the relative pion-nucleon motion denoted E_q.

$$E_q = \sqrt{m_N^2 c^4 + (\hbar c)^2 q^2} + \sqrt{m_\pi c^4 + ()\hbar c)^2 q^2} - m_N c^2 - m_\pi c^2. \tag{2.15}$$

The density of states around q is given by

Looking at (2.12) we want to get an expression for the final state momentum in terms of the wave number

$$\mathrm{d}\rho_f = \frac{Vq}{(2\pi)^3} \frac{1}{2} \frac{\mathrm{d}q^2}{\mathrm{d}E_q} \mathrm{d}\Omega_q. \tag{2.16}$$

We now solve for $(\hbar c)^2 q^2$ in 2.15, which yields the following result

$$(\hbar c)^2 q^2 = \frac{E_q(E_q + 2m_N c^2)(E_q + 2m\pi c^2)(E_q + 2m_N c^2 + 2m_\pi c^2)}{4(E_q + m_N c^2 + m_\pi c^2)^2}, \tag{2.17}$$

and we are now able to calculate the derivative from equation (2.17)

$$\begin{aligned}(\hbar c)^2 \frac{\mathrm{d}q^2}{\mathrm{d}E_q} = &\frac{(E_q^2 + 2E_q m_N c^2 + 2m_N^2 c^4 + 2E_q m_\pi c^2 + 2m_N m_\pi c^4)}{2(E_q + m_N c^2 + m_\pi c^2)^3} \\ &\times \frac{(E_q^2 + 2E_q m_N c^2 + 2m_\pi^2 c^4 + 2E_q m_\pi c^2 + 2m_N m_\pi c^4)}{2(E_q + m_N c^2 + m_\pi c^2)^3},\end{aligned} \tag{2.18}$$

which yields the final expression for the relativistic density of states by plugging equation (2.18) into equation (2.16).

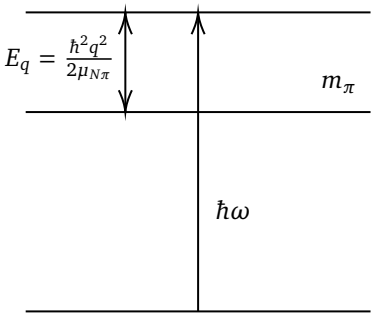

Figure 2.2: Energy diagram of the system. Here $\mu_{N\pi}$ is the reduced mass of the pion-nucleon system

Chapter 3

The nuclear model with explicit mesons

We consider a nuclear model where the nucleus is held together by emitting and absorbing mesons, and the mesons are treated explicitly [2]. We are considering the regime of low-energy nuclear physics, and this model is different from conventional interaction models in several ways. Firstly, the nucleons interact by emitting and absorbing mesons and not via a phenomenological potential. Conceptually this is similar to the one-boson-exchange model. Secondly, the number of parameters is greatly reduced. Regardless of the meson type, the number of parameters is two; the range and the strength of the meson-nucleon coupling are denoted b and S, respectively. In the case of the pion, the central force, tensor force and the three-body force are all concealed within these two parameters. This model should be able to reproduce phenomena within the realm of low-energy nuclear physics, such as the deuteron, nucleon-nucleon scattering, pion-nucleon scattering and pion photoproduction. The low energy regime also enables the use of the Schrödinger equation to describe the equations of motion. The model must be constructed in a way such that usual quantum numbers are conserved; this means conservation of isospin, angular momentum and parity.

3.1 Nuclear interacting model with explicit pions

In the following, we focus on the nuclear model with explicit pions. The pion is the lightest of the strongly interacting particles with a mass of about 15% of the nucleon mass. This yields a large Compton wavelength of 1.4 fm, which means the most extended contribution to nucleon-nucleon interactions. Furthermore, the pion is a significant component of the nuclear wave function where the pion dominates meson exchange corrections to different nuclear properties. In general, the bare nucleon is surrounded by several virtual pions. They are virtual in the same sense that the positron-electron pair are virtual in pair creation from a photon. It is important to stress that these are virtual since they can have properties possible for true particles. The multi-component wave function of the nucleon can be written as

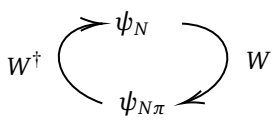

Figure 3.1: Illustration of the pion-nucleon operator, W

$$\Psi_N = \begin{bmatrix} \psi_N \\ \psi_{N\pi} \\ \psi_{N\pi\pi} \\ \vdots \end{bmatrix}, \tag{3.1}$$

where ψ_N is the bare nucleon, and the other wave functions are dressed by an arbitrary number of pions indicated by the subscripts. Assuming the nuclear interaction conserved isospin, angular momentum and parity, we can construct the following operator for the pion-nucleon operator

$$W \equiv (\boldsymbol{\tau} \cdot \boldsymbol{\pi})(\boldsymbol{\sigma} \cdot \mathbf{r}) f(r) \tag{3.2}$$

$$W^\dagger \equiv \int_V \mathrm{d}^3 r \, (\boldsymbol{\tau} \cdot \boldsymbol{\pi})^\dagger (\boldsymbol{\sigma} \cdot \mathbf{r})^\dagger f(r), \tag{3.3}$$

where $\boldsymbol{\tau}$ is the isovector of Pauli matrices acting on the nucleon in isospin space and $\boldsymbol{\sigma}$ is the same but for spin space and $\mathbf{r}$ is the relative coordinate distance between the nucleon and the pion. These operators ensure the conservation of isospin, angular momentum and parity. The isovector of pions is denoted $\boldsymbol{\pi}$ and can be combined with $\boldsymbol{\tau}$ and be represented as a traceless 2-by-2 hermitian matrix given by

$$\boldsymbol{\tau} \cdot \boldsymbol{\pi} = \tau_0 \pi_0 + \sqrt{2}\tau_- \pi^+ \sqrt{2}\tau_+ \pi^- = \begin{bmatrix} \pi^0 & \sqrt{2}\pi^- \\ \sqrt{2}\pi^+ & -\pi^0 \end{bmatrix}, \tag{3.4}$$

where the isospin coefficients will be important later when we discuss different photoproduction processes. Similarly, by expanding the matrices in spin space and using the spherical tensor operator, we get the following matrix in terms of the spherical harmonics

$$\boldsymbol{\sigma} \cdot \mathbf{r} = \sqrt{\frac{4\pi}{3}} r \begin{bmatrix} Y_1^0 & \sqrt{2}Y_1^{-1} \\ \sqrt{2}Y_1^1 & Y_1^0 \end{bmatrix}, \tag{3.5}$$

where similar to in isospin space, the off-diagonals include a factor $\sqrt{2}$.

There is also a phenomenological, short-range form factor $f(r)$ given by

$$f(r) = \frac{S}{b} \mathrm{e}^{-r^2/b^2}, \tag{3.6}$$

where S and b are the pion-nucleon coupling strength and range, respectively–these are illustrated in figure 3.2. The action of annihilating a pion must include the integral over coordinate space to remove the coordinate. We now have everything we need to construct a general Hamiltonian for the multi-component wave function of the nucleon in (3.1)

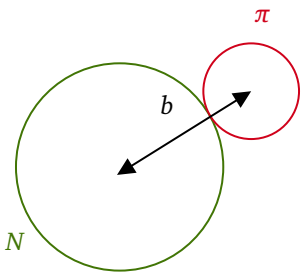

Figure 3.2: Schematic figure of the system to describe the form factor, (3.6). The pion is assumed to sit on the surface.

$$H = \begin{bmatrix} K_N & W^\dagger & 0 & \dots \\ W & K_N + K_\pi + m_\pi c^2 + V_C & W^\dagger & \dots \\ 0 & W & K_N + K_{\pi(1)} + K_{\pi(2)} + 2m_\pi c^2 + V_C & \dots \\ \vdots & \vdots & \vdots & \ddots \end{bmatrix}, \tag{3.7}$$

where the kinetic operators are given by

$$K_N = \frac{-\hbar^2}{2m_N c^2} \frac{\partial}{\partial \mathbf{R}^2} \tag{3.8}$$

$$K_\pi = \frac{-\hbar^2}{2m_\pi c^2} \frac{\partial}{\partial \mathbf{r}^2}. \tag{3.9}$$

Note the different derivatives–here $\mathbf{R}$ is the centre-of-mass coordinate, and $\mathbf{r}$ is the relative coordinate. The subscripts on the kinetic operators in (3.7) represent the order in which the pions are created. Should there be charged particles involved, one must include a Coulomb interaction denoted by V_C. From (3.1) and (3.7) we can construct the general Schrödinger equation

$$H\Psi_N = E\Psi_N, \tag{3.10}$$

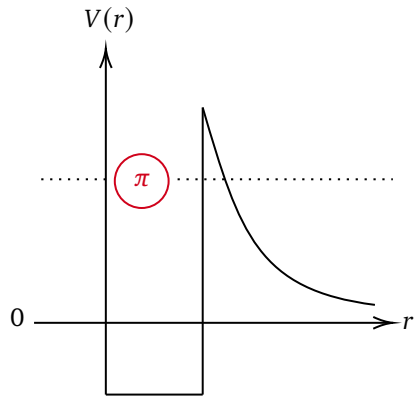

Figure 3.3: Illustration of the virtual pion

where the ground state is the bare nucleon surrounded by virtual pions. The ground state energy in the rest frame of the nucleon gives the mass of the physical nucleon. Within the framework of this model, one can generate a physical pion by supplying enough energy such that the pion is no longer virtual. The pion is trapped behind a potential barrier of height $m_\pi c^2 = 140$ MeV and cannot leave unless this or more energy is supplied to the system.

3.2 Dressing of the nucleon in the one pion approximation

We now consider the scenario where a photon interacts with the nucleon-pion systems and generates a physical pion. This means the energy is higher than the potential barrier also when taking recoil effects into account. This also hints at how a pion photoproduction process would emerge naturally as a disintegration process in this nuclear model. To generate more pions, the photon energy would have to be increased by the same amount. This also means one could assume the first pion is responsible for the largest contribution to the nucleon dressing. This will be referred to as the one-pion approximation. As a proof-of-concept, we constrain ourselves to the one pion approximation and adding more pions should in principle be a straight forward extension of the following calculations.

Returning to (3.1) and enforcing the one-pion approximation yields

$$\Psi = \begin{bmatrix} \psi_N(\mathbf{R}) \\ \psi_{N\pi}(\mathbf{r}) \end{bmatrix}. \tag{3.11}$$

The Hamiltonian which acts on the two-component wave function in (3.11) is given by[1]

$$H = \begin{bmatrix} K_N & W^\dagger \\ W & K_N + K_\pi + m_\pi c^2 \end{bmatrix}, \tag{3.12}$$

So far we have kept the model as simple as possible by expressing the equations in terms of the nucleon. From now on we treat the nucleon of two states of the same strongly interacting object with an intrinsic degree of freedom which defines the proton and neutron. We choose the proton and neutron as

$$|p\rangle = \begin{bmatrix} 1 \\ 0 \end{bmatrix} \quad |n\rangle = \begin{bmatrix} 0 \\ 1 \end{bmatrix}. \tag{3.13}$$

Furthermore, we denote the spin state of the nucleon by an arrow

$$\uparrow = \begin{bmatrix} 1 \\ 0 \end{bmatrix} \quad \downarrow = \begin{bmatrix} 0 \\ 1 \end{bmatrix}. \tag{3.14}$$

The wave function must also be normalized to one nucleon per unit volume. This is as far as we get in general terms for the dressing of the nucleon in the one-pion approximation.

3.3 Dressing of the proton

We now focus our attention on the dressing of the proton in the spin-up state. The calculations are almost identical remembering the definitions from section 3.2. The wave function of the bare proton can thus be written as

$$\psi_p = \frac{p\uparrow}{\sqrt{V}} \tag{3.15}$$

1. Strictly speaking one should use a three-component wave function to account for the mass difference between π^0 and $\pi^\pm$. This is done in appendix C.

The Hamiltonian (3.12) suggest the following expression for the wave function of the pion-nucleon system

$$\psi_{N\pi} = (\boldsymbol{\tau}\cdot\boldsymbol{\pi})(\boldsymbol{\sigma}\cdot\mathbf{r})\frac{p\uparrow}{\sqrt{V}}\phi(r), \tag{3.16}$$

where $\phi(r)$ is the radial function which will play an integral part in the rest of this section. From (3.2) we can construct the Schrödinger equation of the system

$$\begin{bmatrix} K_p & W^\dagger \\ W & K_N + K_\pi + m_\pi c^2 \end{bmatrix}\begin{bmatrix} \psi_p \\ \psi_{N\pi} \end{bmatrix} = E\begin{bmatrix} \psi_p \\ \psi_{N\pi} \end{bmatrix}. \tag{3.17}$$

Note that the kinetic operator in the second row still contains K_N to emphasise that this acts on the general nucleon-pion wave function, $\psi_{N\pi}$. Expanding (3.17) yields two equations

$$K_p\psi_p + W^\dagger\psi_{N\pi} = E\psi_p \tag{3.18}$$

$$W\psi_p + (K_N + K_\pi + m_\pi c^2)\psi_{N\pi} = E\psi_{N\pi}. \tag{3.19}$$

In the rest frame of the proton the center-of-mass dependency vanishes and inserting the operator (3.2) yields

$$\int_V \mathrm{d}^3r\,(\boldsymbol{\tau}\cdot\boldsymbol{\pi})^\dagger(\boldsymbol{\sigma}\cdot\mathbf{r})^\dagger f(r)\phi(r)(\boldsymbol{\tau}\cdot\boldsymbol{\pi})(\boldsymbol{\sigma}\cdot\mathbf{r})p\frac{1}{\sqrt{V}} = Ep\frac{1}{\sqrt{V}}, \tag{3.20}$$

where the integration comes from equation (3.3). This can be further simplified using relations for the matrix vectors[2]

2. $(\boldsymbol{\tau}\cdot\boldsymbol{\pi})^\dagger(\boldsymbol{\tau}\cdot\boldsymbol{\pi}) = 3$ and $(\boldsymbol{\sigma}\cdot\mathbf{r})^\dagger(\boldsymbol{\sigma}\cdot\mathbf{r}) = r^2$

$$12\pi\int_0^\infty \mathrm{d}r\, f(r)\phi(r)r^4 = E. \tag{3.21}$$

Similarly for (3.19) where the term $K_N\psi_{N\pi}$ vanishes,

$$\begin{aligned}(\boldsymbol{\tau}\cdot\boldsymbol{\pi})(\boldsymbol{\sigma}\cdot\mathbf{r})f(r)p\frac{1}{\sqrt{V}} - \frac{\hbar^2}{2\mu_{N\pi}}\nabla^2_{\mathbf{r}}(\boldsymbol{\tau}\cdot\boldsymbol{\pi})(\boldsymbol{\sigma}\cdot\mathbf{r})p\frac{1}{\sqrt{V}}\phi(r) \\ = (E - m_\pi c^2)(\boldsymbol{\tau}\cdot\boldsymbol{\pi})(\boldsymbol{\sigma}\cdot\mathbf{r})\phi(r)p\frac{1}{\sqrt{V}},\end{aligned} \tag{3.22}$$

using (3.9) and where $\mu_{N\pi}$ is the reduced mass of the nucleon-pion system. This equation can be further simplified by using a vector operator relation which yields[3]

3. $\nabla^2(\mathbf{r}\phi(r)) = \mathbf{r}\left(\frac{\mathrm{d}^2\phi(r)}{\mathrm{d}r^2} + \frac{4}{r}\frac{\mathrm{d}\phi(r)}{\mathrm{d}r}\right)$

$$f(r) - \frac{\hbar^2}{2\mu_{N\pi}}\left(\frac{\mathrm{d}^2\phi(r)}{\mathrm{d}r^2} + \frac{4}{r}\frac{\mathrm{d}\phi(r)}{\mathrm{d}r}\right) = (E - m_\pi c^2)\phi(r). \tag{3.23}$$

This means equation (3.21) and (3.23) are the two equations that must be solved numerically.

$$\left.\begin{aligned} &12\pi\textstyle\int_0^\infty \mathrm{d}r\, f(r)\phi(r)r^4 = E \\ &f(r) - \frac{\hbar^2}{2\mu_{N\pi}}\left(\frac{\mathrm{d}^2\phi(r)}{\mathrm{d}r^2} + \frac{4}{r}\frac{\mathrm{d}\phi(r)}{\mathrm{d}r}\right) + m_\pi c^2\phi(r) = E\phi(r)\end{aligned}\right\} \tag{3.24}$$

The bracket on the right is used to empathise that (3.24) is a coupled system.

3.4 Numerical considerations

To solve the system of equations (3.24) one can consider two different numerical approaches. One approach gives a more intuitive picture of

how to solve this kind of equation while the other is more robust and practical.

For a given E one can solve the second-order differential equation corresponding to $\phi[E]$. Conversely, for a given $\phi(r)$ one can calculate the integral to find $E[\phi]$. This leads to the fixed-point equation given by

$$E[\phi[\mathcal{E}]] = \mathcal{E}, \tag{3.25}$$

which is a single variable non-linear equation. Equation (3.25) can be solved using a root-finding algorithm. This approach is generally not as efficient since the algorithm will have to search through large parameter space to find a suitable solution.

The second approach consists of reformulating the system (3.24) as a boundary value problem with the following conditions

$$I'(r) = 12\pi f(r)\phi(r)r^4, \quad I(0) = 0,\ I(\infty) = E. \tag{3.26}$$

Essentially, what is written in equation 3.26 is the boundary conditions we require for the energy. The equation starts from a singular point and extends to an infinite point. We require the solution to stay finite which means approximations are needed at both limits. At $r \to 0$ the differential equation is approximately an Euler-Cauchy equation with basis solutions 1 and r^{-1}. For finite solutions the latter is ignored which means $\phi'(a) = 0$ is the requirement for $a \approx 0$.[4] For $r \to \infty$ the dominating term in the differential equation is

$$-\phi''(r) + 2\mu_{N\pi}(m_\pi c^2 - E)\phi(r) = 0. \tag{3.27}$$

Since we expect a negative value for E the basis solutions are on the form

$$\phi(r) = \exp\left\{\pm\sqrt{2\mu_{N\pi}(m_\pi c^2 + |E|)}\right\}r. \tag{3.28}$$

In the case of a positive sign, the solution diverges. For the basis solution with negative exponents, we have

$$\phi'(r) + \sqrt{2\mu_{N\pi}(m_\pi c^2 + |E|)}\phi(r) = 0. \tag{3.29}$$

These two conditions are suitable boundary conditions for the left and right boundaries, respectively. The algorithm converges and a solution to (3.17) is found. The solutions can be seen in figure 3.4 for the parameters $S = 10$ MeV and $b = 1$ fm.

4. You would end up with the same conclusion if you consider $\phi = a + r^n$ and plug this into $\phi'' + 4\phi'/r = 0$, which yields $n = 0, -1$.

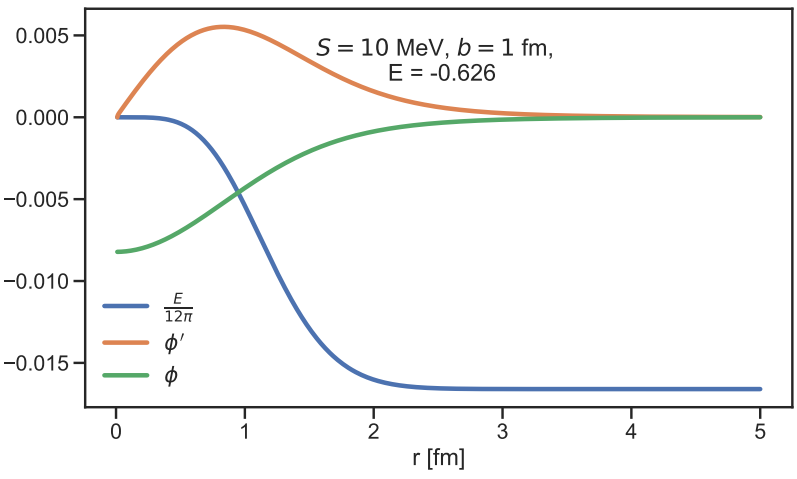

Figure 3.4: Boundary value problem solutions. The plot is generated using a tolerance of 10^{-6}. The blue line representing the energy is scaled.

Also, note that since we expect the energy to be less than zero it makes sense for the wave function to be negative since all other terms in the integral in equation (3.24) are positive. It might appear strange to have a negative wave function, $\phi(r)$ but there are two things to note. One can add an arbitrary phase to equation (3.11) and flip the sign. Also for all calculations, we are only interested in the norm-square of the wave function. The energy for the parameters shown in figure 3.4 is $E = -0.626\,\text{MeV}$ and this value is very sensitive to the parameters S and b since they enter in the form factor as seen in equation (3.6) and as mentioned in section 3.1 this gives the physical mass of the proton–it's importance will be clear later when comparing the discussion the mass contribution from virtual pion in section 4.

Since we cannot allow the wave function to extend to infinity numerically we must introduce some cut-off. Since the wave function of the pion-nucleon system has a built-in range parameter b it is natural to let the cut-off be proportional to this parameter. Within the regime of nuclear physics, we expect the wave function to extend up to a length within the order of magnitude of ten Fermi. Quantitatively this means a small constant of proportionality $O(0.01)$ in front of r_{min} and another constant $O(1)$ in front of r_{max}. Numerically, a constant of proportionality for r_{max} and the impact can be seen on figure 3.5 where the radial wave functions stop after $5r_{\text{max}}$.

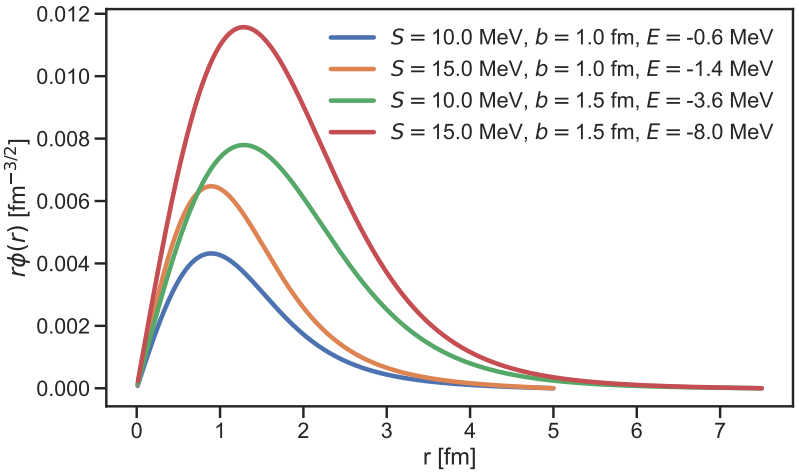

Figure 3.5: Radial wave function for different parameters S and b to illustrate the behavoir on the radial function.

Figure 3.5 also illustrates the behaviour of the radial wave functions as the parameters change. As the coupling strength parameter S increases the radial wave function increases. As the range parameter b increases the peak is shifted to this new value. Also, note the unit of the radial wave function. We know the following integral must be dimensionless

$$\int_V \mathrm{d}^3R \int_V \mathrm{d}^3r \left|\psi_{N\pi}\right|^2, \tag{3.30}$$

which means the wave function $\phi(r)$ must have dimensions of $\text{fm}^{-5/2}$ and the radial wave function $r\phi(r)$ must have dimensions of $\text{fm}^{-3/2}$. Note here the two integrals come from the annihilation of a pion and the normalization of one particle per unit volume respectively.

3.4.1 Different form factors

Compared to conventional interaction models of the nucleus this model has the advantage of having very few parameters. The phenomenological

form factor $f(r)$ only consists of an interaction strength S and a range parameter b. The form factor can take many different forms yielding different wave function solutions which in turn changed the energy. The formalism in 3.4 is very flexible so changes in the form factor and here we explore how different form factors impact the wave function. The form factors must all decrease as a function of r since we constrain the system to short-range forces. The solutions on figure 3.5 assumes the form factor from equation 3.6 which is Gaussian. A priori we do now know anything about the form factor and it might as well be Yukawa like

$$f(r) = \frac{S}{b}\frac{\exp\left\{-\frac{r}{b}\right\}}{r}. \tag{3.31}$$

Figure **??** shows the radial wave functions if the form factor is Yukawa like

Figure 3.6:

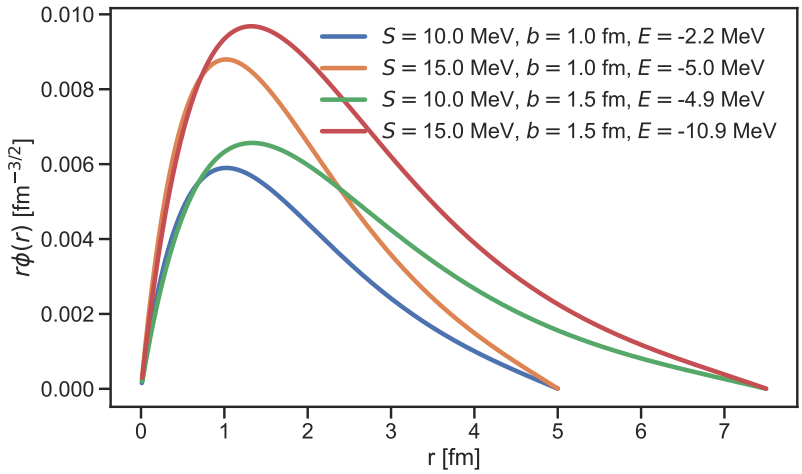

The shapes of the radial wave functions are similar to the Gaussian case but the energies do not match due to the r^2/b^2 dependency in the Gaussian case. One could argue for a Yukawa-like form factor but with a gaussian exponential and the energies are the same within a few MeV but this defeats the purpose of a Yukawa form. An exponential form factor would make the radial wave function too long to describe the nuclear range since we are constrained to about 15 fm.

3.4.2 Relativistic Expansion

As described in section 3.1 we are using the Schrödinger equation which hints at a non-relativistic limit of the pion-nucleon system. We also know the pion is virtual which means under a potential barrier. An avant-garde idea is to do relativistic expansion of the kinetic term which depends on the relative coordinate **r**.

The pion is virtual which makes the velocity of the particle hard to estimate–nonetheless we can do an expansion of the kinetic operator and see how this affects the model. To account for relativistic effects we can replace the kinetic term, $K_{\mathbf{r}}$ in (3.17)

$$K_{\mathbf{r}} \to K_{\mathbf{r},\text{rel}} = \sqrt{p^2c^2 + \mu_{N\pi}^2 c^4} = \mu_{N\pi}c^2\left(\sqrt{1 + \frac{p^2}{\mu_{N\pi}^2 c^2}} - 1\right), \tag{3.32}$$

where $\mu_{N\pi}$ is the reduced mass of the nucleon-pion system. This leads to a new system of equations and these solutions can be compared to the

non-relativistic limit to deduce which relativistic regime dominates the system. Starting from (3.19)

$$f(r)(\boldsymbol{\tau}\cdot\boldsymbol{\pi})(\boldsymbol{\sigma}\cdot\mathbf{r})\psi_p + \mu_{N\pi}c^2\left(\sqrt{1+\frac{p^2}{\mu_{N\pi}^2c^2}}-1\right)\psi_{N\pi} = (E-m_\pi c^2)\psi_{N\pi}, \tag{3.33}$$

This equation turns out to be divergent and we must therefore resort to an approximation. The kinetic energy is expanded

$$K_{\mathbf{r},\mathrm{rel}} = \mu_{N\pi}c^2\sqrt{1+\frac{p^2}{\mu_{N\pi}^2}} - \mu_{N\pi}c^2 \approx \frac{p^2}{2\mu_{N\pi}} - \frac{p^4}{8\mu_{N\pi}^3c^2} \tag{3.34}$$

This means we get an extra term in (3.22) yielding

$$\begin{aligned}(\boldsymbol{\tau}\cdot\boldsymbol{\pi})(\boldsymbol{\sigma}\cdot\mathbf{r})f(r)\frac{p\uparrow}{\sqrt{V}} + \left(\frac{p^2}{2\mu_{N\pi}} - \frac{p^4}{8\mu_{N\pi}^3c^2}\right)(\boldsymbol{\tau}\cdot\boldsymbol{\pi})(\boldsymbol{\sigma}\cdot\mathbf{r})\frac{p\uparrow}{\sqrt{V}}\phi(r)\\ = (E-m_\pi c^2)(\boldsymbol{\tau}\cdot\boldsymbol{\pi})(\boldsymbol{\sigma}\cdot\mathbf{r})\phi(r)\frac{p\uparrow}{\sqrt{V}},\end{aligned} \tag{3.35}$$

Using the vector operators yields the following expression[5]

$$\begin{aligned}f(r) - \frac{\hbar^2}{2\mu_{N\pi}}\left(\phi^{(2)}(r)+\frac{4}{r}\phi^{(1)}(r)\right) - \frac{\hbar^4}{8\mu_{N\pi}^3c^3}\left(\phi^{(4)}(r)+\frac{6}{r}\phi^{(3)}(r)\right)\\ = (E-m_\pi c^2)\phi(r),\end{aligned} \tag{3.36}$$

where the exponent, (n), is the order of the differentiation. This leads to a system of equations given by

$$\left.\begin{array}{l} 12\pi\int_0^\infty \mathrm{d}r\, f(r)\phi(r)r^4 = E \\ f(r) - \frac{\hbar^2}{2\mu_{N\pi}}\left(\phi^{(2)}(r)+\frac{4}{r}\phi^{(1)}(r)\right) - \frac{\hbar^4}{8\mu_{N\pi}^3c^3}\left(\phi^{(4)}(r)+\frac{6}{r}\phi^{(3)}(r)\right) = (E-m_\pi c^2)\phi(r)\end{array}\right\} \tag{3.37}$$

This system is a fourth-order differential equation coupled to an integrodifferential equation and is solved using the boundary value problem technique. The boundary conditions can be found using the same considerations as in the previous section. For $r\to\infty$ the dominating terms are

$$\phi^{(4)}(r) = \frac{-8\mu_{N\pi}c^2}{\hbar^4}(E-m_\pi c^2)\phi(r) - \frac{4\mu_{N\pi}^2c^2}{\hbar^2}\phi(r)^{(2)} \tag{3.38}$$

The solutions are shown in figure 3.7 where only $\phi(r)$ and $\phi(r)^{(1)}$ are included

5. $$\nabla^4(\mathbf{r}\phi(r)) = \mathbf{r}\left(\phi^{(4)}+\frac{6}{r}\phi^{(3)}\right)$$

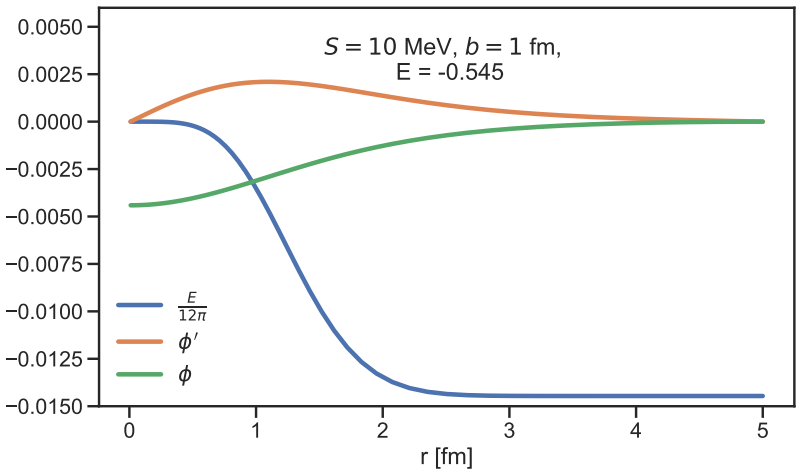

Figure 3.7: Boundary value problem solutions for the relativistic expansion. The plot is generated using a tolerance of 10^{-3}. The energy convergence is scaled.

We gain information about the system both from the wave function and the energy and we consider these two components of figure 3.7 separately. The radial wave function of the system can be seen in figure 3.8

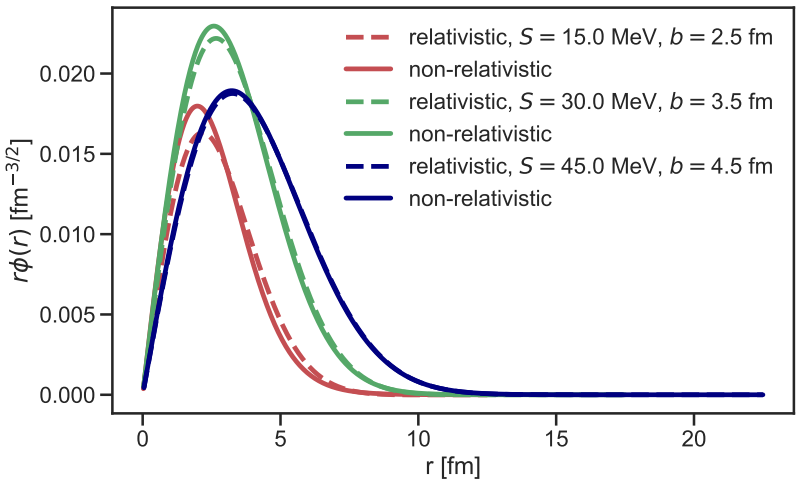

Figure 3.8: Relativistic (dashed) and non-relativistic radial wave functions for three different parameters. The matching colours have the same parameters

The radial wave functions are similar with the lowest strength parameter S and range parameter b having the largest difference. This can be explained by considering equation (3.37). The form factor $f(r)$ depends explicitly on the ratio between these two parameters in the same way in the relativistic limit as in the non-relativistic limit. However, the form factor can change by orders of magnitude by varying the two parameters and this will only affect the solution $\phi(r)$ regarding when the form factor vanishes and the $r \to \infty$ limit applies. This also means we should expect the energy ratio between the non-relativistic equation (3.24) and equation (3.37) to approach 1 as the range parameter b increases since this decreases the impact of the form factor. This is shown in figure 3.9 where the energy ratio is given by

$$E_R = \frac{E_{\text{relativistic}}}{E_{\text{non-relativistic}}}. \tag{3.39}$$

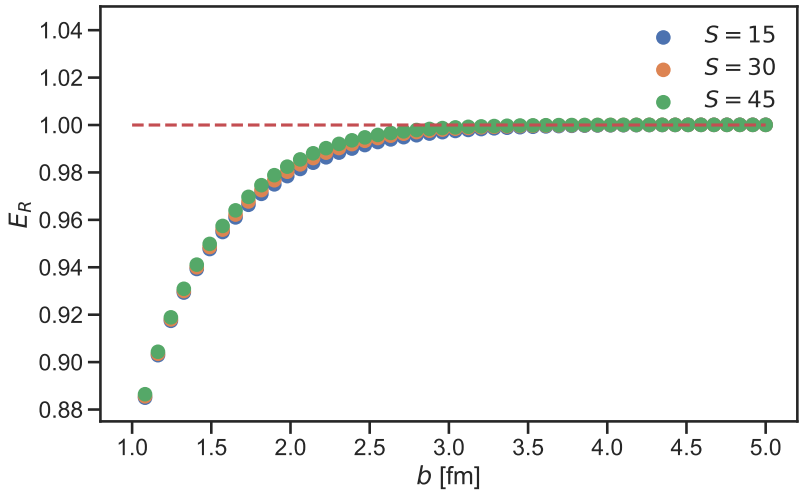

Figure 3.9: The energy ratio $E_{\text{rel}}/E_{\text{nonrel}}$ shown as a function of the range parameter b for a Gaussian form factor given by equation (3.6)

We can apply the same logic to the system of equations with a Yukawa-like form factor as in equation (3.31) and we expect the same convergence. This is shown on figure 3.10

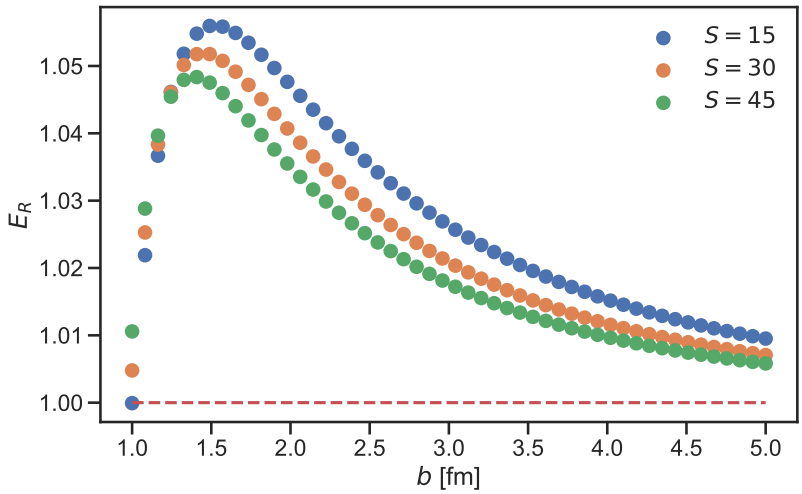

Figure 3.10: The energy ratio $E_{\text{rel}}/E_{\text{nonrel}}$ shown as a function of the range parameter b for a Yukawa-like form factor given by equation (3.31)

The pion is virtual and hence in a classically forbidden region but we can still estimate which relativistic regime dominates the system. Both in terms of the radial wave function and in terms of the energy ratio relativistic effects are negligible. This result holds for different form factors since they most all decrease a function of r.

Considering figure 3.9 we see the maximum discrepancy between the relativistic and the non-relativistic energy is about 10 percent and decreases rapidly. This means relativistic effects vanish as we increase the range parameter b. A physical explanation of this could be that as we increase the spatial dimension a virtual pion with the same kinetic energy would have a lower velocity and hence less relativistic. This analysis is supported if the same behaviour is not present when we hold b fixed an increase S since. This is shown on figure 3.11 for the Gaussian form factor

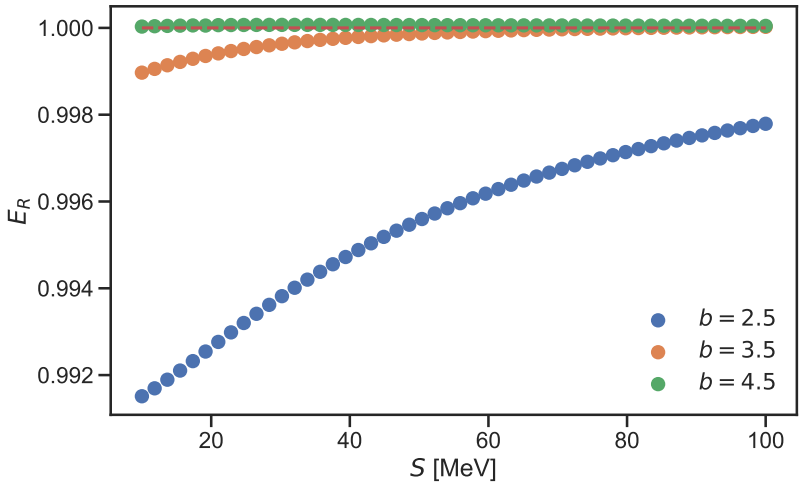

Figure 3.11: The energy ratio $E_{\text{rel}}/E_{\text{nonrel}}$ shown as a function of the strength parameter b for a Yukawa-like form factor given by equation (3.31)

A similar plot for the Yukawa-like form factor

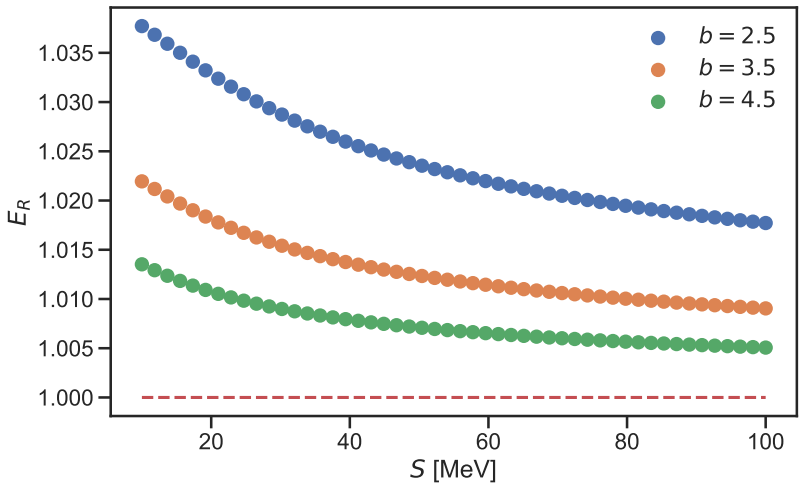

Figure 3.12: The energy ratio $E_{\text{rel}}/E_{\text{nonrel}}$ shown as a function of the strength parameter S for a Yukawa-like form factor given by equation (3.31)

3.4.3 Nuclear Effective Field Theory operator

The construction of the most general chiral Lagrangian is based on the theory of the non-linear realization of symmetry. The baryon-number-conserving chiral Lagrangian can be split into pieces with even numbers of fermion fields where in this section we will focus on

$$\mathcal{L} = N^\dagger \left(i\mathcal{D}_0 + \frac{\boldsymbol{\mathcal{D}}^2}{2m_N} \right) N + \frac{g_A}{2f_\pi} N^\dagger \boldsymbol{\tau} N \cdot \mathbf{D}\boldsymbol{\pi}, \tag{3.40}$$

where the second term is very similar to the creation operator W from equation (3.2)–only the $\mathbf{r}$ is replaced by $\nabla_{\mathbf{r}}$. The general operator is constructed in such a way that parity, isospin and spin are conserved and there is some freedom in the choice of the distance operator. In this section, we explore the differences, if any, by constructing the nuclear model with explicit mesons with the operator as is it defined in chiral effective field theory. We assume the following form of the wave function of the proton and the system consisting of a nucleon and a single pion

$$\psi_p = p \uparrow \frac{1}{\sqrt{V}}, \quad \psi_{N\pi} = (\boldsymbol{\tau} \cdot \boldsymbol{\pi})(\boldsymbol{\sigma} \cdot \frac{\partial}{\partial \mathbf{r}}) p \uparrow \frac{1}{\sqrt{V}} \phi, \tag{3.41}$$

where $\boldsymbol{\tau}$ and $\boldsymbol{\sigma}$ are vectors consisting of Pauli matrices acting on isospin and spin space on the nucleon respectively. $\boldsymbol{\pi}$ is the isovector of pions. We now construct an operator to create and annihilate a pion

$$W = (\boldsymbol{\tau} \cdot \boldsymbol{\pi})(\boldsymbol{\sigma} \cdot \frac{\partial}{\partial \mathbf{r}}) f(r) \tag{3.42}$$

$$W^\dagger = \int_V \mathrm{d}^3 r \, (\boldsymbol{\tau} \cdot \boldsymbol{\pi})^\dagger (\boldsymbol{\sigma} \cdot \frac{\partial}{\partial \mathbf{r}})^\dagger f(r), \tag{3.43}$$

where $f(r)$ is a form factor. The annihilation operator must contain the integral to remove the coordinate of the pion. This leads to the following Schrödinger equation

$$\begin{bmatrix} K_{\mathbf{R}} & W^\dagger \\ W & K_{\mathbf{R}} + K_{\mathbf{r}} + m_\pi c^2 \end{bmatrix} \begin{bmatrix} \psi_p \\ \psi_{N\pi} \end{bmatrix} = E \begin{bmatrix} \psi_p \\ \psi_{N\pi} \end{bmatrix}, \tag{3.44}$$

which is expanded

$$12\pi \int_0^\infty \mathrm{d}r \, \frac{\partial^2}{\partial r^2} r^2 f(r) \phi(r) = E \tag{3.45}$$

$$\frac{\partial}{\partial r} f(r) - \frac{2\hbar^2}{\mu_{N\pi}} \frac{\partial^3}{\partial r^3} \phi(r) = (E - m_\pi c^2) \frac{\partial}{\partial r} \phi(r). \tag{3.46}$$

Assume the form factor is on the following form

$$f(r) = \frac{S}{b} \mathrm{e}^{-r^2/b^2} \tag{3.47}$$

which yields

$$\frac{\partial}{\partial r} f(r) = \frac{-2r}{b^2} f(r), \quad \frac{\partial^2}{\partial r^2} = -\frac{2(b^2 - 2r^2 2)}{b^4} f(r). \tag{3.48}$$

The terms inside the integral in equation (3.45)

$$\frac{\partial^2}{\partial r^2}(r^2 f(r)\phi(r)) = 2rf(r)\phi(r) + 2rf'(r)\phi(r) + r^2 f(r)\phi'(r) \tag{3.49}$$

$$+ 2rf'(r)\phi(r) + r^2 f''^{(r)}\phi(r) + r^2 f'(r)\phi'(r) \tag{3.50}$$

$$+ 2rf(r)\phi(r) + r^2 f'(r)\phi'(r) + r^2 f(r)\phi''(r) \tag{3.51}$$

$$\equiv Y(r) \tag{3.52}$$

Considering the limits of (3.46) which for large r is

$$\phi'''(r) = \frac{-\mu_{N\pi}}{2\hbar^2}(E - m_\pi c^2)\phi'(r) \tag{3.53}$$

The solution is shown on 3.13

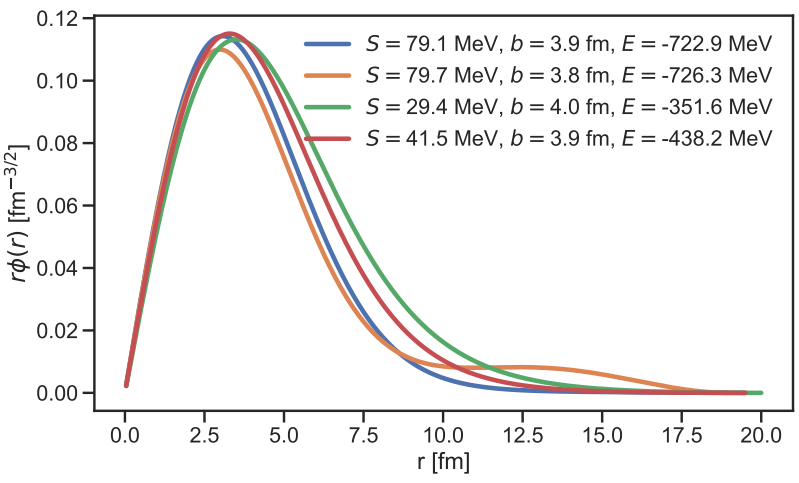

Figure 3.13: The radial wave function using the operator form from an effective field theory.

The parameters S and b in the radial wave functions are not the same as in figure 3.5 and figure 3.6 but should better represented actual parameter values when performing the fit to the total cross-section data. This is done to better highlight the validity of this model and some of it's disadvantages. The energies are within the same order of magnitude as when using the model as described in section 3.3. There is a difference in energy and this model could be investigated further – however, this model using the operator from nuclear effective field theory is a lot more intensive numerically. Due to the derivative in equation (3.41), (3.42) and (3.43) we got many more terms as seen in (3.52) which all have to be integrated numerically. Perhaps another numerical method is better suited for this operator type.

3.4.4 Charge density

Using

$$\rho_q(\mathbf{r}_{\mathrm{rm}}) = q_1 \int \mathrm{d}^3 r_\pi \mathrm{d}^3 r_N \left|\psi(r_\pi, r_N)\right|^2 \delta(\mathbf{r}_{\boldsymbol{\pi}} - \mathbf{R}, \mathbf{r}_{\mathrm{cm}}) \tag{3.54}$$

$$= q_1 \int \mathrm{d}^3 r_\pi \mathrm{d}^3 r_N \left|\psi(\mathbf{R} + \frac{m_N}{M}\mathbf{r}, \mathbf{R} - \frac{m_\pi}{M}\mathbf{R})\right|^2 \delta(\mathbf{R} + \frac{m_n}{M}\mathbf{r} - \mathbf{R}, \mathbf{r}_{\mathrm{cm}}) \tag{3.55}$$

$$= q_1 \int \mathrm{d}^3 R \left|r\psi(\frac{m_N}{M}\mathbf{r}_{cm})\right|^2 \tag{3.56}$$

$$= q_1 \left|\mathbf{r}\phi(\frac{m_N}{M}\mathbf{r}_{\mathrm{cm}})\right|^2 \tag{3.57}$$

Chapter 4

Pion photoproduction

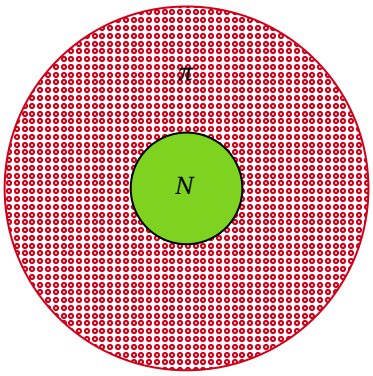

Figure 4.1: Illustration of the dressed nucleon. In the centre (green) is a nucleon and surrounding it is a cloud of virtual pions (red gradient).

We now consider the case of pion photoproduction. In the model mentioned in section 3.1 the nucleon is in a superposition of states with an arbitrary number of pions but we constrain the model to the one-pion approximation. This is illustrated on figure 4.1

There are four pion photoproduction processes on nucleons and these are given by

$$p\gamma \longrightarrow p\pi^0 \tag{4.1}$$
$$p\gamma \longrightarrow n\pi^+ \tag{4.2}$$
$$n\gamma \longrightarrow n\pi^0 \tag{4.3}$$
$$n\gamma \longrightarrow p\pi^-. \tag{4.4}$$

Within the framework of this model, we would expect these processes by applying the equation (3.4) to the isospin state of the given nucleon, i.e

$$(\boldsymbol{\tau}\cdot\boldsymbol{\pi})p = p\pi^0 + \sqrt{2}n\pi^+, \tag{4.5}$$

and similarly for the isospin state of the neutron. As mentioned in section 3.3 the pion is trapped behind a potential barrier of height 140 MeV and cannot leave unless an incoming photon of sufficient energy hits the pion-nucleon system and photodisintegrates the virtual pion and creates a physical pion in the process. This means pion photoproduction comes naturally as a photodisintegration process. Consider some initial bound state represented by the following two-component wave function

$$|\Phi_i\rangle = \begin{bmatrix} \phi_p \\ \phi_{N\pi} \end{bmatrix}, \tag{4.6}$$

where ϕ represents a bound state. The final state consists of the same superposition but in an unbound system represented by ψ, i.e.

$$|\Psi_f\rangle = \begin{bmatrix} \psi_p \\ \psi_{N\pi} \end{bmatrix}. \tag{4.7}$$

The two-component wave function photodisintegration is similar to the photodisintegration process of the deuteron[1]. We can apply a similar approach and get an expression for the total cross section as a function of energy and the strength parameter S and the range parameter b. The general idea is to fit the parameters to experimental data such that we get a set of parameters within which the model can describe the total cross-section near the threshold. We constrain the model to only apply near the threshold since we expect more pions are needed to adaquatly describe the total cross section at higher energies. The advantages of this

1. This is covered in appendix A

model are twofold–the reduced number of parameters allows us to easily fit the model to experimental data and the generality of the model allows us to apply these parameters to a different process accounting only for the difference in mass and isospin coefficient. Also, in the case of pion photoproduction process (4.1) is very well investigated experimentally while (4.2) and (4.1) have limited data and (4.3) have none near the threshold. Our first approach is to apply a dipole approximation since we are considering the photoproduction processes near the threshold.

4.1 Dipole Approximation

We want to calculate the total cross-section of pion photoproduction off nucleons. In this section, we focus on the process involving charged pions off protons given by equation (4.2). The general idea is to use Fermi's golden rule, and this involves a matrix element expressed in terms of equation (4.6) and equation (4.7) can be described as

$$\left\langle \Psi_f \middle| \mathbf{d} \middle| \Phi_i \right\rangle, \tag{4.8}$$

where a dipole operator $\mathbf{d}$. We start from the general expression of the multi-component wave function and impose a normalisation to both the initial and final state. Starting from (4.6)

$$\Phi = \mathcal{N}\begin{bmatrix} p\uparrow \\ (\boldsymbol{\tau}\cdot\boldsymbol{\pi})(\boldsymbol{\sigma}\cdot\mathbf{r})p\uparrow \phi(r) \end{bmatrix}, \tag{4.9}$$

where $\uparrow$ represents the spin state, $\phi(r)$ is the wave function from figure 3.4 and $\mathcal{N}$ is the normalization constant. This leads to

$$\begin{aligned} \langle\Phi|\Phi\rangle &= |\mathcal{N}|^2 \left(\left\langle \phi_p \middle| \phi_p \right\rangle + \left\langle \phi_{N\pi} \middle| \phi_{N\pi} \right\rangle \right) && (4.10)\\ &= |\mathcal{N}|^2 \left(V + 3V \int \mathrm{d}^3 r\, r^2 \phi(r)^2 \right) && (4.11)\\ &\stackrel{!}{=} 1. && (4.12) \end{aligned}$$

This leads to the following normalisation constant

$$\mathcal{N} = \frac{1}{\sqrt{V}} \frac{1}{\sqrt{1+\epsilon}}, \tag{4.13}$$

where V is the volume and ϵ is the integral in (4.11)–numerically, this is close to unity. This expression is the properly normalised initial state.

The final state consists of the unbound system represented by ψ. We know the final state consists of a plane wave with wave number $\mathbf{q}$ propagating along the z-axis. This can be represented by

$$\mathrm{e}^{iqz} = \mathrm{e}^{i\mathbf{q}\cdot\mathbf{r}}, \tag{4.14}$$

where θ is the angle between $\mathbf{q}$ and $\mathbf{r}$ illustrated on 4.2. Using orthogonality and the addition theorem for the spherical harmonics, we can decompose the plane wave into a Bessel function and spherical harmonics[2]. This yields

$$\begin{aligned} \frac{1}{\sqrt{V}} \mathrm{e}^{-i\mathbf{q}\cdot\mathbf{r}} &= \frac{1}{\sqrt{V}} \sum_{\ell,m} 4\pi i^\ell Y_\ell^{*m}(\mathbf{q}) Y_\ell^m(\mathbf{r})\, j_\ell(qr) && (4.15)\\ &= \frac{1}{\sqrt{V}} \sum_{\ell} 4\pi i^\ell j_\ell(qr) \left(\frac{2\ell+1}{4\pi} \right) P_\ell(\cos\theta), && (4.16) \end{aligned}$$

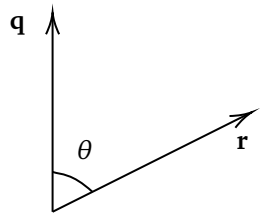

Figure 4.2: Illustration of the angle between the two vectors $\mathbf{q}$ and $\mathbf{r}$ in equation (4.17)

2. This is proved in appendix B.1

and P_ℓ is the Legendre polynomial of degree ℓ. Since we are considering the energies close to the threshold, we expect mainly the S-wave to contribute and ignore higher orders. We should empathise that this is an approximation, and a priori, we do not know to what degree this holds. In terms of the expansion (4.15) this greatly reduces the expression

$$\frac{1}{\sqrt{V}} e^{i\mathbf{q}\cdot\mathbf{r}} \overset{\ell=0}{=} \frac{1}{\sqrt{V}} j_0(qr). \tag{4.17}$$

As equation (4.17) shows, we are left with a spherical Bessel function in the final state where the volume is kept to stress that according to (REF MISSING) the total cross section must be independent of the volume. Considering the S-wave channel for the following process $p\gamma \to n\pi^+$ yields the following matrix element

$$\mathcal{M} = -i\omega_k \sqrt{\frac{2\pi\hbar}{V\omega_\mathbf{k}}} \mathbf{e}_{\mathbf{k},\lambda} \left\langle \frac{1}{\sqrt{V}} j_0(qr) n\pi^+(\uparrow\downarrow) |\mathbf{d}| (\boldsymbol{\tau}\cdot\boldsymbol{\pi})(\boldsymbol{\sigma}\cdot\mathbf{r}) p\uparrow \phi(r)\mathcal{N} \right\rangle \tag{4.18}$$

where the two arrows represent the two spin states of the neutron and the proton. The front factor arises from the normalisation factor in front of the 2nd quantisation operator. The different spin states of the neutron in the final state yield two contributions to the total matrix element given by

$$\begin{aligned}
\mathcal{M}^\uparrow &= \frac{-i\mathcal{N}\sqrt{2}\omega_k \mathbf{e}_{\mathbf{k},\lambda}}{V} \sqrt{\frac{2\pi\hbar}{V\omega_\mathbf{k}}} \langle j_0(qr)|d_0 r_0|\phi(r)\rangle && (4.19)\\
&= \frac{-i\mathcal{N}\sqrt{2}\omega_k \mathbf{e}_{\mathbf{k},\lambda}}{V} \sqrt{\frac{2\pi\hbar}{V\omega_\mathbf{k}}} \sqrt{\frac{4\pi}{3}} \langle j_0(qr)|d_0 r Y_1^0|\phi(r)\rangle && (4.20)\\
\mathcal{M}^\downarrow &= \frac{-i\mathcal{N}2\omega_k \mathbf{e}_{\mathbf{k},\lambda}}{V} \sqrt{\frac{2\pi\hbar}{V\omega_\mathbf{k}}} \left\langle j_0(qr)\middle|dr_+\middle|\phi(r)\right\rangle && (4.21)\\
&= \frac{-i\mathcal{N}2\omega_k \mathbf{e}_{\mathbf{k},\lambda}}{V} \sqrt{\frac{2\pi\hbar}{V\omega_\mathbf{k}}} \sqrt{\frac{4\pi}{3}} \langle j_0(qr)|d_0 r Y_1^1|\phi(r)\rangle\,, && (4.22)\\
& && (4.23)
\end{aligned}$$

where the spin-down state picks up a factor $\sqrt{2}$ from equation (3.5). Now we calculate the remaining matrix elements,

$$\begin{aligned}
\left\langle j_0(qr)\middle|d_0 r_0\middle|\phi(r)\right\rangle &= \frac{\mu}{m_\pi} e \left\langle j_0(qr)\middle|r_0 r_0\middle|\phi(r)\right\rangle && (4.24)\\
&= \frac{\mu}{m_\pi} e \frac{4\pi}{3} \left\langle j_0\middle|r^2\middle|\phi(r)\right\rangle && (4.25)\\
&= \frac{\mu e}{m_\pi} \int_0^\pi \int_0^{2\pi} \int_0^\infty \mathrm{d}r\mathrm{d}\phi\mathrm{d}\theta\, j_0(qr) r^4 \cos^2\theta \sin\theta \phi(r) && (4.26)\\
&= \frac{4\pi\mu e}{3m_\pi} \underbrace{\int_0^\infty \mathrm{d}r\, j_0(qr) r^4 \phi(r)}_{Q(r)}, && (4.27)
\end{aligned}$$

where the dipole operator has been inserted and the angular integrals calculated. We have also introduced an integral, which contains the wave

function $\phi(r)$. Similarly, for the next matrix element,

$$\left\langle j_0(qr)\middle|d_- r_+\middle|\phi(r)\right\rangle = \frac{\mu}{m_\pi} e \left\langle j_0(qr)\middle|r_- r_+\middle|\phi(r)\right\rangle \tag{4.28}$$

$$= \frac{4\pi\mu e}{3m_\pi}\left\langle j_0(qr)\middle|r^2 Y_1^{-1} Y_1^1\middle|\phi(r)\right\rangle \tag{4.29}$$

$$= \frac{4\pi\mu e}{3m_\pi} Q. \tag{4.30}$$

It turns out these two matrix elements are equal. Taking the norm-square of (4.27)

$$\left|\mathcal{M}^\uparrow\right|^2 = \left(\frac{4\pi\mu e}{3m_\pi}\right)^2 \frac{2\mathcal{N}^2\omega_k(2\pi\hbar)}{V^2}(\mathbf{e}_{\mathbf{k},\lambda})^0(\mathbf{e}^*_{\mathbf{k},\lambda})^0 Q^2 \tag{4.31}$$

Similarly, for the equation (4.30)

$$\left|\mathcal{M}^\downarrow\right|^2 = \left(\frac{4\pi\mu e}{3m_\pi}\right)^2 \frac{4\mathcal{N}\omega_{\mathbf{k}}(2\pi\hbar)}{V^2}(\mathbf{e}_{\mathbf{k},\lambda})^+(\mathbf{e}^*_{\mathbf{k},\lambda})^+ Q^2. \tag{4.32}$$

3. $(\mathbf{e}^*_{\mathbf{k},\lambda}\cdot\mathbf{e}_{\mathbf{k},\lambda}) = \delta_{\lambda,\lambda'}$ and $\mathbf{e}_{\mathbf{k},\mp} = \pm\frac{1}{\sqrt{2}}(\mathbf{e}_{\mathbf{k},1} \pm i\mathbf{e}_{\mathbf{k},2})$. This leads to $(\mathbf{e}^{0*}_{\mathbf{k},\lambda}\cdot\mathbf{e}^0_{\mathbf{k},\lambda'}) + (\mathbf{e}^{0+}_{\mathbf{k},\lambda}\cdot\mathbf{e}^+_{\mathbf{k},\lambda'}) = \delta_{\lambda,\lambda'} + \frac{1}{2}\delta_{\lambda,\lambda'}$

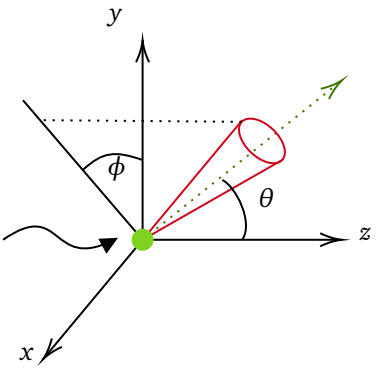

Figure 4.3: Illustration of the differential cross-section.

Calculating the total matrix element using a polarization theorem[3]

$$|\mathcal{M}|^2 = \left|\mathcal{M}^\uparrow\right|^2 + \left|\mathcal{M}^\downarrow\right|^2 \tag{4.33}$$

$$= \frac{2\pi\hbar\omega_k\mathcal{N}^2e^2}{V^2}\left(\frac{4\pi\mu}{3m_\pi}\right)^2 Q^2, \tag{4.34}$$

which is the final expression for the matrix element. According to Fermi's golden rule, we can calculate the transition probability

$$\mathrm{d}\omega = \frac{2\pi}{\hbar}|\mathcal{M}|^2\,\mathrm{d}\rho, \tag{4.35}$$

where the density of states is given by

$$\mathrm{d}\rho = \frac{Vqm}{\hbar^2(2\pi)^3}\mathrm{d}\Omega. \tag{4.36}$$

To go from the transition probability to the differential cross-section, we need to consider the flux density of the photons. This means a factor V/c, where V is the volume, and c is the speed of light. This leads to the final expressions for the differential cross-section.

$$\frac{\mathrm{d}\sigma}{\mathrm{d}\Omega_q} = \frac{16\pi}{9}\mathcal{N}^2\alpha\frac{kq\mu_{N\pi}^3}{m_\pi^2\hbar c}Q^2, \tag{4.37}$$

and since there is no explicit angular dependency, the total cross-section is given by

$$\sigma_{\text{dipole}} = \oint_{4\pi}\frac{\mathrm{d}\sigma}{\mathrm{d}\Omega_q}\mathrm{d}\Omega_q \tag{4.38}$$

$$= 4\pi\frac{16\pi}{9}\mathcal{N}^2\alpha\frac{kq\mu_{N\pi}^3}{m_\pi^2\hbar c}Q^2 \tag{4.39}$$

$$= \frac{64\pi^2}{9}\mathcal{N}^2\alpha\frac{kq\mu_{p\pi}^3}{m_\pi^2\hbar c}\left(\int_0^\infty \mathrm{d}r\; j_0(qr)r^4\phi(r)\right)^2. \tag{4.40}$$

This is the final expression for the total cross-section of photoproduction of charged pions using the dipole approximation. We now perform a fit to experimental data for the parameters S and b and enter in the wave

function $\phi(r)$. Here two considerations are needed. Both the dipole approximation and the one-pion approximation limit the validity of the cross-section to near the threshold. And due to the limited amount of experimental data for charged pion photoproduction the fit is limited to approximately 15 MeV from the threshold. This means some data points are excluded to constrain the fitted parameters to values that might seem physically realistic.

The fit is performed and can be seen in figure 4.4.

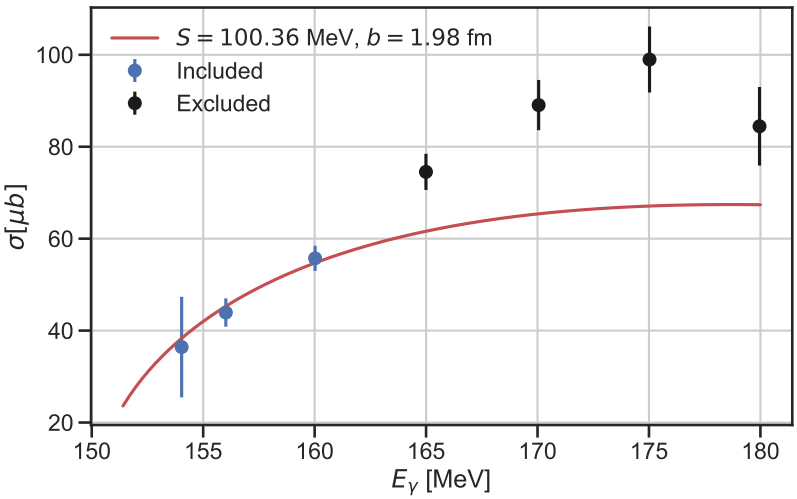

Figure 4.4: The total cross-section of the photoproduction process $\gamma p \to \pi^+ n$ fitted to experimental data. The fit parameters are shown in the figure. The blue data points are included in the fit, and the black data points are excluded since these violate both the dipole and the one pion approximation.

The parameters S and b seem reasonable, but more importantly, we are interested in the relative weight coming from the $N\pi$ component in the wave function and the virtual pions' contribution to the dressed proton. This corresponds to solving the equations in (3.24) with the new parameters. The contribution to the wave function is calculated as follows

$$\int_V \mathrm{d}^3R \int_V \mathrm{d}^3r \left|\psi_{N\pi}\right|^2 = 4\pi \int_0^\infty \mathrm{d}r\, \phi(r)^2 r^2 \tag{4.41}$$

$$= 0.69 \tag{4.42}$$

using (3.16) and considering only the π^+ component in $\boldsymbol{\pi}$. The energy is calculated which yields

$$E_{\text{virtual pions}} = -449\,\text{MeV}. \tag{4.43}$$

Note here that we have used two approximations that limit (4.40) to energies very close to the threshold. To further test the validity of the model, we need a more general expression for the cross-section and more data points. This means we have to consider the exact matrix element for the transition and consider the photoproduction of neutral pions off protons since this is the most experimentally investigated photoproduction process.

4.2 Exact Matrix Element

In section 4.1 we looked at how to use the model described in section 3.1 to get an expression for the cross-section which was compared to experimental data. More specifically we used the dipole approximation which introduces a trade-off between the difficulty of the calculations and the regime in which our solution is valid. We expect the dipole approximation to hold for low energies just above the threshold. To both

validate and generalize this result we now do a different approach and calculate the cross-section exact and also consider recoil effects. Strictly speaking, recoil effects should also be considered in section 4.1 since the mass ratio between the nucleon and the pion cannot be assumed to yield a stationary nucleon after the pion photoproduction process. To calculate the exact matrix elements we consider a non-relativistic system of particles interacting with the electromagnetic field. The interacting part of the Hamiltonian is given by

$$H = \frac{1}{2m_\pi}\left(\mathbf{p} - \frac{e}{c}\mathbf{A}(\mathbf{r})\right)^2, \tag{4.44}$$

where $\mathbf{p}$ is the momentum operator and $\mathbf{A}(\mathbf{r})$ is the quantized vector potential at the point $\mathbf{r}$. Note that we have already replaced the usual mass by the mass of the pion, m_π since we are considering the interaction of a pion with charge e with the electromagnetic field.

The electromagnetic interaction is relatively weak compared to the strong force. For our problem, this means we can expand the interaction by taking only the lowest non-vanishing order of perturbation into account. Since we later want to consider transition probabilities we only keep the first non-linear term of (4.44) which yields

$$V^{(1)} = -\frac{e}{2m_p c}\Big(\mathbf{p}\cdot\mathbf{A}(\mathbf{r}_p,t) + \mathbf{A}(\mathbf{r}_p,t)\cdot\mathbf{p}\Big), \tag{4.45}$$

which also means the interacting part is linear in the creation(annihilation) operators corresponding to single-photon emission(absorption). Our choice of gauge is purely conventional and we choose the radiation gauge which imposes a condition on the vector potential given by

$$\nabla\cdot\mathbf{A} = 0, \tag{4.46}$$

and this is a convenient choice of gauge since the commutator in (4.45) is $\nabla\cdot\mathbf{A}$ and we can write

$$V^{(1)} = -\frac{e}{m_p c}\mathbf{A}(\mathbf{r_p},t)\cdot\mathbf{p}_p. \tag{4.47}$$

Note that (4.47) consists of the pion momentum operator, $\mathbf{p}_\pi$ and the electromagnetic vector potential at a distance r_π. This distance was also mentioned in section 3.1 and can be expressed in term of the Jacobi coordinates illustrated on figure 4.5 where the relative coordinate is given by $\mathbf{r} = \mathbf{r}_\pi - \mathbf{r}_p$ which leads to the following transformation of equation (4.47)

$$V^{(1)} = -\frac{e}{m_p c}\mathbf{A}(\mathbf{r_p},t)\cdot\mathbf{p}_p = -\frac{e}{m_p c}\mathbf{A}\left(\mathbf{R} - \frac{m_\pi}{M_{p\pi}}\mathbf{r},t\right)\left(\frac{m_p}{M_{p\pi}}\mathbf{P} - \mathbf{p}\right), \tag{4.48}$$

where $M_{p\pi} = m_p + m_\pi$ is the total mass of the system and $\mathbf{R}$ is the coordinate vector for the center of mass. We now move on from the general theory of the pion interacting with the electromagnetic field and consider the specific case of pion photoproduction. To recap we consider the following processes

$$p\gamma \to p\pi^0 \tag{4.49}$$
$$p\gamma \to n\pi^+ \tag{4.50}$$
$$n\gamma \to n\pi^0 \tag{4.51}$$
$$n\gamma \to p\pi^-, \tag{4.52}$$

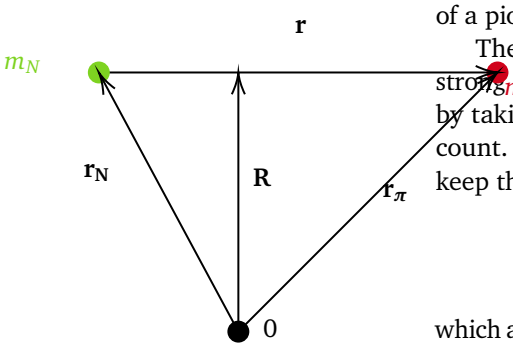

Figure 4.5: Jacobi coordinates illustrating $\mathbf{r}_\pi$ used in the vector potential in equation 4.47. Here we use $\mathbf{r} = \mathbf{r}_\pi - \mathbf{r}_p$ and see that $\mathbf{r}_\pi = \mathbf{R} + \mathbf{r}\frac{m_p}{M_{p\pi}}$, where $M_{p\pi} = m_p + m_\pi$.

where the initial states consist of a dressed proton or neutron and a plane wave photon which in the language of 2nd quantization can be written as $a^\dagger_{\mathbf{k},\lambda}|0\rangle$ corresponding to creating a photon with wave vector $\mathbf{k}$ and polarization λ from the vacuum $|0\rangle$. The final states consists of a nucleon and a pion and no photon, i.e electromagnetic vacuum. This leads to the following expression for the matrix element for the transitions in (4.49), (4.50), (4.51) and (4.52)

$$\frac{-e}{m_\pi c}\langle 0|\mathbf{A}\big(\mathbf{R}-\frac{m_\pi}{M_{p\pi}}\mathbf{r},t\big)a^\dagger_{\mathbf{k},\lambda}|0\rangle = \frac{-e}{m_p}\sqrt{\frac{2\pi\hbar}{\omega_\mathbf{k}V}}\mathbf{e}_{\mathbf{k},\lambda}e^{i\mathbf{k}(\mathbf{R}-\frac{m_\pi}{M_{p\pi}}\mathbf{r})-i\omega_k t}. \tag{4.53}$$

Completely analogous to section **??** and specifically equation (4.35) we now want to consider the probability of transition per unit time of going from the initial state $|i\rangle$ to $\langle f|$ according to Fermi's golden rule

$$\mathrm{d}\omega = \frac{2\pi}{\hbar}|\mathcal{M}|^2\,\mathrm{d}\rho, \tag{4.54}$$

where $\mathrm{d}\rho$ is the density of states also analogous to (4.36). The difference is that we do not employ the dipole approximation to evaluate the matrix element $\mathcal{M}$ and we also consider recoil. In the following section we focus on pion photoproduction of neutral pion off protons corresponding to the transition in (4.49). The choice is due to the fact that there is a lot more experimental data available for pion photoproduction off protons compared to neutrons since it is easier to achive experimentally. We focus on neutral pions since our one-pion approximation is assumed to be valid near the threshold and since we are interested in fitting to experimental data we need as much data near the threshold as possible–and this is the case for neutral pion photoproduction

4.2.1 Neutral Pion Phototoproduction off Protons

From (4.53) we get

$$\mathcal{M}^{(\uparrow\downarrow)} = \frac{e}{m_p}\sqrt{\frac{2\pi\hbar}{\omega_\mathbf{k}V}}\langle(\uparrow\downarrow)p\pi^0|\frac{e^{i\mathbf{q}\cdot\mathbf{r}}}{\sqrt{V}}\frac{e^{i\mathbf{Q}\cdot\mathbf{r}}}{\sqrt{V}}|e^{i\mathbf{k}(R-\frac{m_\pi}{M_{p\pi}}\mathbf{r})}(\mathbf{e}_{\mathbf{k},\lambda}\mathbf{p})|(\boldsymbol{\tau}\cdot\boldsymbol{\pi})(\boldsymbol{\sigma}\cdot\mathbf{r})\phi(r)\frac{p\uparrow}{\sqrt{V}}\rangle \tag{4.55}$$

$$= \frac{-e}{m_p}\sqrt{\frac{2\pi\hbar}{\omega_\mathbf{k}V}}\langle(\uparrow\downarrow)\frac{e^{i\mathbf{q}\cdot\mathbf{r}}}{\sqrt{V}}\frac{e^{i\mathbf{Q}\cdot\mathbf{r}}}{\sqrt{V}}|e^{i\mathbf{k}(R-\frac{m_\pi}{M_{p\pi}}\mathbf{r})}(\mathbf{e}_{\mathbf{k},\lambda}\mathbf{p})|(\boldsymbol{\sigma}\cdot\mathbf{r})\phi(r)\frac{\uparrow}{\sqrt{V}}\rangle\,, \tag{4.56}$$

where we have used $\int \mathrm{d}^3r e^{i\mathbf{k}\cdot\mathbf{R}} = V$ and $\langle p\pi^0|\boldsymbol{\tau}\cdot\boldsymbol{\pi}|p\rangle = 1$. Note that $\mathbf{q}$ is the wave-number of the pion-proton relative momentum and $\mathbf{Q}$ is originates from conservation of momentum, that is $\mathbf{Q} = \mathbf{k}$. Defining a new vector, $\mathbf{s} = \mathbf{q} + \frac{m_\pi}{M_{p\pi}}\mathbf{k}$ yields

$$\mathcal{M}^{(\uparrow\downarrow)} = \frac{-e}{m_\pi}\sqrt{\frac{2\pi\hbar}{\omega_\mathbf{k}}}\frac{1}{V}\langle(\uparrow\downarrow)|\langle e^{i\mathbf{s}\cdot\mathbf{r}}|(\mathbf{e}_{\mathbf{k},\lambda}\mathbf{p})(\boldsymbol{\sigma}\cdot\mathbf{r})|\phi(r)\rangle|\uparrow\rangle \tag{4.57}$$

Note the different inner products. We now do the plane wave expansion using (4.15) and consider the angular averaging of two coordinates variables[4]

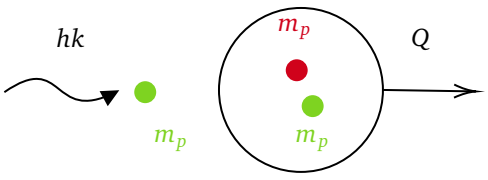

Figure 4.6: Neutral pion photoproduction with conservation of momentum $\mathbf{k} = \mathbf{Q}$ illustrated

4. $\int \mathrm{d}\Omega\, n_k n_l = \frac{4\pi}{3}\delta_{kl}$, which means $\int \mathrm{d}\Omega\, r_k r_l = \frac{4\pi r^2}{3}\delta_{kl}$, where n is a unit vector

$$\langle e^{i\mathbf{s}\cdot\mathbf{r}}|(\mathbf{e}_{\mathbf{k},\lambda}\frac{\partial}{\partial\mathbf{r}})(\boldsymbol{\sigma}\cdot\mathbf{r})|\phi(r)\rangle = +i(\mathbf{e}_{\mathbf{k},\lambda}\cdot\mathbf{s})\int \mathrm{d}^3r\, e^{i\mathbf{s}\cdot\mathbf{r}}(\boldsymbol{\sigma}\cdot\mathbf{r})\phi(r) \quad (4.58)$$

$$= -i(\mathbf{e}_{\mathbf{k},\lambda}\cdot\mathbf{s})\int \mathrm{d}^3r\, 3ir j_1(sr)\frac{\mathbf{s}\cdot\mathbf{r}}{sr}(\boldsymbol{\sigma}\cdot\mathbf{r})\phi(r) \quad (4.59)$$

$$= (\mathbf{e}_{\mathbf{k},\lambda}\cdot\mathbf{s})(\boldsymbol{\sigma}\cdot\mathbf{r})\underbrace{\frac{4\pi}{s}\int_0^\infty \mathrm{d}r\, r^3 j_1(sr)\phi(r)}_{F(s)} \quad (4.60)$$

$$= (\mathbf{e}_{\mathbf{k},\lambda}\cdot\mathbf{s})(\boldsymbol{\sigma}\cdot\mathbf{r})F(s). \quad (4.61)$$

Returning to the matrix element (4.56)

$$\mathcal{M}^{(\uparrow\downarrow)} = \frac{ie\hbar}{m_p}\sqrt{\frac{2\pi\hbar}{\omega_k}}\frac{1}{V}\langle(\uparrow\downarrow)|(\mathbf{e}_{\mathbf{k},\lambda}\cdot\mathbf{s})F(s)|\uparrow\rangle \quad (4.62)$$

$$= \frac{ie\hbar}{m_p}\sqrt{\frac{2\pi\hbar}{\omega_k}}\frac{1}{V}(\mathbf{e}_{\mathbf{k},\lambda}\cdot\mathbf{s})\,\langle(\uparrow\downarrow)|(\boldsymbol{\sigma}\cdot\mathbf{r})|\uparrow\rangle\,F(s), \quad (4.63)$$

5. We do this step already to use a completeness relation for the polarization.

which leads to the following expression for the norm square[5]

$$\left|\mathcal{M}^{(\uparrow\downarrow)}\right|^2 = \frac{2\pi\hbar^3e^2}{m_p^2\omega_kV^2}\left|\mathbf{e}_{\mathbf{k},\lambda}\cdot\mathbf{s}\right|^2\left|\langle(\uparrow\downarrow)|(\boldsymbol{\sigma}\cdot\mathbf{r})|\uparrow\rangle\right|^2F(s)^2, \quad (4.64)$$

and now calculating

$$\sum_\lambda = \left|(\mathbf{e}_{\mathbf{k},\lambda}\cdot\mathbf{s})\right|^2 = \sum_\lambda(\mathbf{e}^*_{\mathbf{k},\lambda}\cdot\mathbf{s})(\mathbf{e}_{\mathbf{k},\lambda}\cdot\mathbf{s}) \quad (4.65)$$

$$= s^2 - \frac{(\mathbf{k}\cdot\mathbf{s})^2}{k^2} \quad (4.66)$$

$$= q^2 - \frac{(\mathbf{k}\cdot\mathbf{q})^2}{k^2} \quad (4.67)$$

$$= q^2\sin^2(\theta_q), \quad (4.68)$$

where θ_q is the angle between $\mathbf{k}$ and $\mathbf{q}$ and we now have an angular dependency originating from the dot product. I have added a subscript q to empathize that this relative to the final state momentum $\mathbf{q}$ located in (θ,ϕ) also illustrated on figure 4.3.

Plugging (4.65) into (4.64) yields

$$\frac{1}{2}\sum_{\lambda,(\uparrow\downarrow)}\left|\mathcal{M}_{fi}\right|^2 = \frac{\pi e^2\hbar^3}{V^2m_p^2}\frac{1}{\omega_k}q^2\sin^2(\theta)s^2F(s)^2. \quad (4.69)$$

According to Fermi's golden rule the transition probability is given by

$$\mathrm{d}\omega = \frac{2\pi}{\hbar}|\mathcal{M}|^2\,\mathrm{d}\rho, \quad \mathrm{d}\rho = \frac{V\mu_{p\pi}q}{\hbar^2(2\pi)^3}\mathrm{d}\Omega_q, \quad (4.70)$$

where the density of states in the final state assumes a non-relativistic expansion. Strictly speaking this is an approximation. Also, $\mathbf{q}$ denotes the differential angle element to empathize that this is relative to the pion-proton system. Plugging (4.69) into (4.70)

$$\mathrm{d}\omega = \frac{e^2}{8\pi}\frac{\mu_{p\pi}c^2}{m_p^2c^4\omega_k}q^3\sin^2(\theta_q)s^2F(s)^2\mathrm{d}\Omega_q \quad (4.71)$$

which leads to the following expression for the differential cross section by considering the time it takes the photon to cross the volume, V.

$$\frac{\mathrm{d}\sigma}{\mathrm{d}\Omega_q} = \frac{e^2}{8\pi}\frac{\mu_{p\pi}c^2}{m_p^2c^4}\frac{q^3}{k}\sin^2(\theta_q)s^2F(s)^2 \tag{4.72}$$

In (4.72) we have an expression for the angular dependency. This means for some photon energy we get an angular distribution. This can also be compared to experimental data. (This can be done for all the figures in [1] and also for charged pions). Figure 4.7 shows the differential cross section as a function of the angle θ_{cm} compared to experimental data.

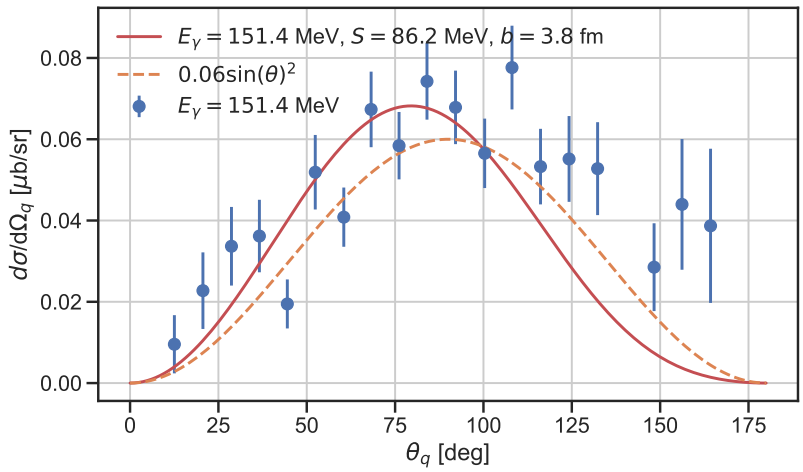

Figure 4.7: Not fitted parameters! Note the dependency is not $\sin(\theta_q)^2$ since there is a contribution from $F(s)$ as well.

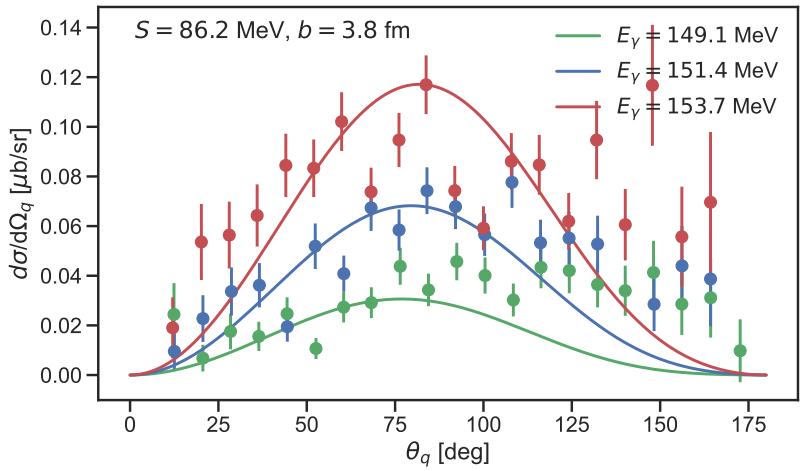

Figure 4.8: Multiple energies

To get an expression for the total cross section equation the expression is integrated into containing only a radial part using

$$\sigma = 2\pi\int_0^\pi \mathrm{d}\theta\,\sin(\theta_q)\frac{\mathrm{d}\sigma}{\mathrm{d}\Omega_q} \tag{4.73}$$

$$= 2\pi\int_0^\pi \mathrm{d}\theta\,\frac{e^2}{8\pi}\frac{\mu_{p\pi}c^2}{m_p^2c^4}\frac{q^3}{k}\sin^3(\theta)s^2F(s)^2 \tag{4.74}$$

(4.73) is fitted to experimental data such that the physical parameters in our model S and b can be extracted. So far the values of these parameters have been chosen at random. However, we do have some intuition about how these two affect the wavefunction of the system from figure **??**. From

(4.73) we see that the wave function only enters explicitly in the integral so the general behavior of the cross section is hard to predict. The fit is done and can be seen in figure 4.9. Data is from [3]

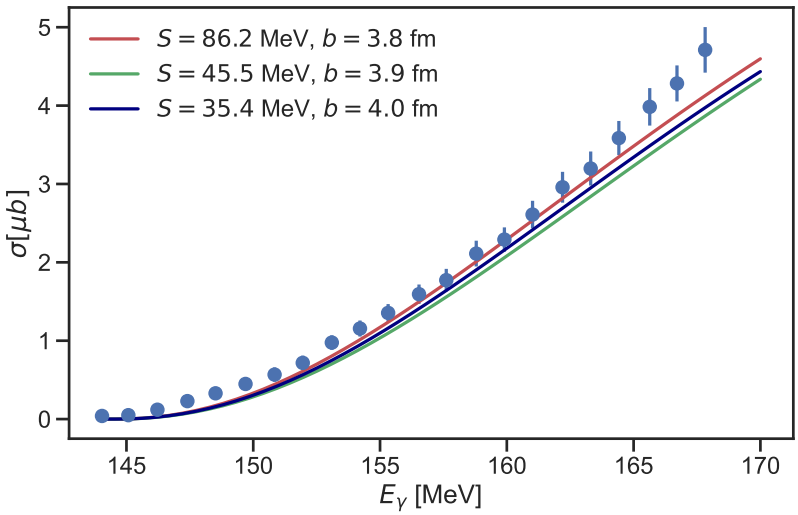

Figure 4.9: Fitted parameters to experimental data for the process $\gamma p \to \pi^0 p$. The fit parameters for S, b are shown inside the figure.

Note that these expressions are for the production of neutral pions. The same approach can be done for charged pions.

There is some freedom of choice in the fit. The integral is slowly converging and a cut-off must be introduced. This cut-off is arbitrary and does affect the fit. For a larger cut-off the line flattens out before 165 MeV. This leads to a more phenomenological discussion of the model in relation to the cross section as a function of energy. For higher energies we expect more than one pion to contribute to the cross section. This model, however, only takes one pion into account. To describe the behavior at higher energies more pions must be taking into account. This highlights the strengths and weaknesses of using differential equations to describe the physical system. If we take more pions into account this approach is no longer favorable since this leads to too many coupled systems. For more pions one would have to resort to another method.

4.2.2 Neutral Pion Phototoproduction off Neutrons

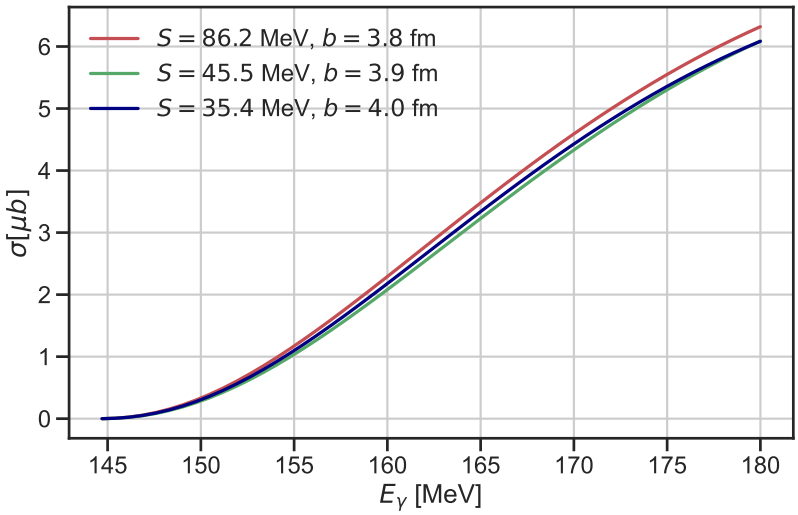

Figure 4.10: The process $\gamma n \to \pi^0 n$ with the same parameters as for neutral pion photoproduction off protons.

4.2.3 Charged Pion Phototoproduction off Protons

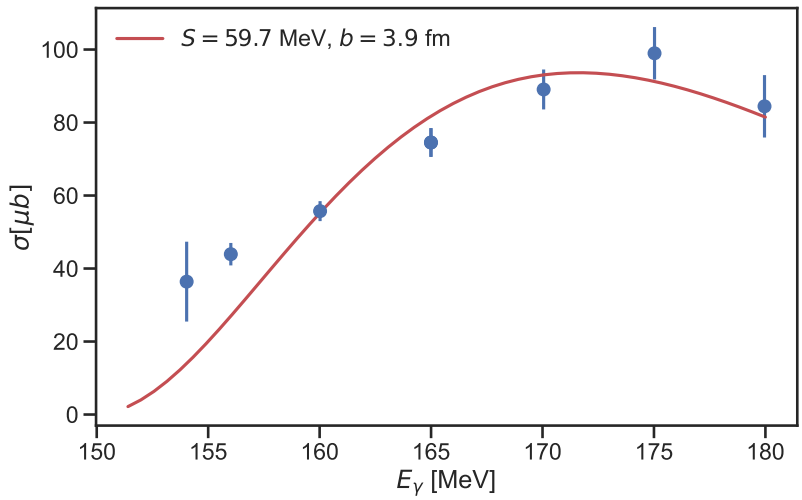

Figure 4.11: d.

4.2.4 Charged Pion Phototoproduction off Neutrons

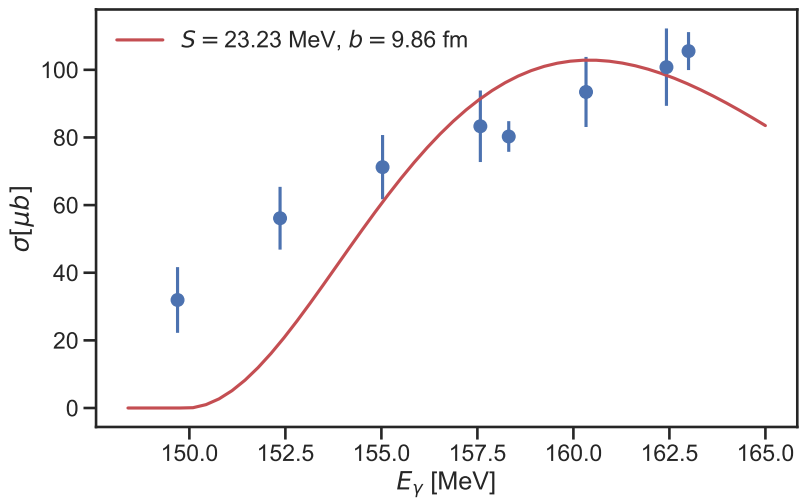

Figure 4.12: d.

Bibliography

[1] R. Beck et al. “Measurement of the p(γ,π^0) cross section at threshold”. In: *Phys. Rev. Lett.* 65 (15 Oct. 1990), pp. 1841–1844. DOI: 10.1103/PhysRevLett.65.1841. URL: https://link.aps.org/doi/10.1103/PhysRevLett.65.1841.

[2] D. V. Fedorov. “A Nuclear Model with Explicit Mesons”. In: *Few-Body Systems* 61.4 (Oct. 2020). ISSN: 1432-5411. DOI: 10.1007/s00601-020-01573-1. URL: http://dx.doi.org/10.1007/s00601-020-01573-1.

[3] A. Schmidt et al. “Test of Low-Energy Theorems for $^1H(\vec{\gamma},\pi^0)^1H$ in the Threshold Region”. In: *Phys. Rev. Lett.* 87 (23 Nov. 2001), p. 232501. DOI: 10.1103/PhysRevLett.87.232501. URL: https://link.aps.org/doi/10.1103/PhysRevLett.87.232501.

[4] Vladimir Zelevinsky and Alexander Volya. *Physics of Atomic Nuclei*. First. Wiley-VCH, 2017.

Appendix A

Nuclear photoeffect and the deuteron

In this appendix, I wish to go through how to get expressions for the differential cross section and the total cross section from the wave function. The wave function can be obtained analytically or numerically – in this appendix, I will sketch an analytical approach to s-wave calculations. Considering the central potential between the proton and the neutron given by

$$U(r) = \begin{cases} -U_0, & r \leq R \\ 0 & r > R \end{cases}$$

The radial equation is given by

$$-\frac{\hbar^2}{2m}\frac{\mathrm{d}^2u(r)}{\mathrm{d}r^2} + \left[U(r) + \frac{\hbar^2\ell(\ell+1)}{2mr^2}\right]u(r) = Eu(r). \tag{A.1}$$

This is identical to the one-dimensional Schrodinger equation with an effective potential, where the centrifugal term pushes the particle outwards. To solve this analytically I rewrite the equation and consider the boundary conditions.

$$\frac{\mathrm{d}^2u(r)}{\mathrm{d}r^2} + \frac{M}{\hbar^2}\left[E - U(r)\right]u(r) = 0, \tag{A.2}$$

where I plugged in the expression for the reduced mass, $m = M/2$. For the deuteron I use $E = -E_B = -2.225$ MeV [4, p. 51]. This leads to the following expressions

$$\frac{\mathrm{d}^2u(r)}{\mathrm{d}r^2} + \frac{M}{\hbar^2}\left(U_0 - E_B\right)u(r) = 0, \quad r \leq R, \tag{A.3}$$

$$\frac{\mathrm{d}^2u(r)}{\mathrm{d}r^2} - \frac{M}{\hbar^2}E_B u(r) = 0, \quad r > R. \tag{A.4}$$

I introduce two variables given by

$$k = \sqrt{\frac{M}{\hbar^2}\left(U_0 - E_B\right)}, \quad \kappa = \sqrt{\frac{ME_B}{\hbar^2}}. \tag{A.5}$$

Rewriting equation (A.3) in terms of (A.5) and solving the differential equation yields

$$\frac{\mathrm{d}^2u(r)}{\mathrm{d}r^2} = -ku(r) \Rightarrow u(r) = A\sin(kr) + B\cos(kr). \tag{A.6}$$

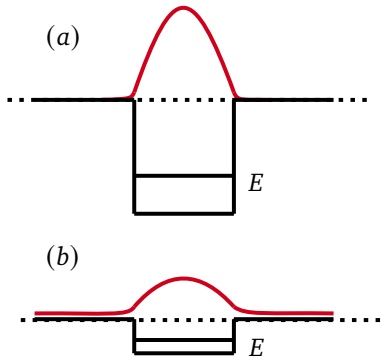

Figure A.1: Behavior of the ground state bound wave function for two potentials. (a) is an illustration of the deeper potential well case and (b) is for a shallower potential well.

Since $R(r) = u(r)/r$ and $\cos(kr)/r$ blows up as $r \to 0 \Rightarrow B = 0$ and the solution is

$$u(r) = A\sin(kr), \quad r \leq R \tag{A.7}$$

Now, considering equation (A.4)

$$\frac{\mathrm{d}^2u(r)}{\mathrm{d}r^2} = \kappa^2 u(r) \Rightarrow u(r) = Ce^{\kappa r} + De^{-\kappa r} \tag{A.8}$$

Here $Ce^{\kappa r}$ blows up as $r \to \infty$. The wavefunction must be continuous and this means the solutions (A.6) and (A.8) must match at $r = R$. The same applies for the derivative. This leads to two equations for $r = R$.

$$A\sin(kR) = De^{-\kappa R} \tag{A.9}$$

$$Ak\cos(kR) = -D\kappa e^{-\kappa R} \tag{A.10}$$

Dividing equation (A.10) by equation (A.9) leads to

$$-\cot(kR) = \frac{\kappa}{k} \tag{A.11}$$

This equation is solved by requiring $kR = \pi/2$. Plugging in an appropiate value for $R = 1.7$ fm yields

$$\begin{aligned} U_0 &= \frac{\hbar^2\pi^2}{2mR^2} - E \\ &= \frac{\hbar^2\pi^2}{2mR^2} + E_B \\ &= 37.2\,\mathrm{MeV} \end{aligned}$$

This means the depth of the potential is 37.2 MeV.

Note that this is all for s-wave. Some considerations about the tensor force are also needed. This means we have to consider the Schrödinger equation with noncentral spin-dependent potential given by

$$\mathcal{U}(r) = \mathcal{U}_0(r) + \mathcal{U}_t(r)S_{12}, \tag{A.12}$$

where

$$\mathcal{U}_t(r) = \mathcal{U}_{tW}(r) + \mathcal{U}_{tM}(r), \tag{A.13}$$

for the space-even states we are considering with the deuteron, see table A. Considering the d-wave I introduce the anglular momentum coupling $[Y_2(\mathbf{n})\chi_1]_{1M}$ of spin 1 and $\ell = 1$ to the total deuteron spin $J = 1$ and projection $J_z = M$. The same coupling but properly normalized can be written as

$$\Theta_M = \frac{1}{\sqrt{32\pi}} S_{12}\chi_{1M}. \tag{A.14}$$

To get the complete wave function of the deuteron the expression must contain two radial parts and a spherical wave factor $1/r$

$$\Psi_M = \frac{1}{\sqrt{4\pi}}\frac{1}{r}\left(u_0(r) + \frac{1}{\sqrt{8}}u_2(r)S_{12}\right)\chi_{1M}, \tag{A.15}$$

where the two radial parts are $u_0(r)$ and $u_2(r)$ for s-wave and d-wave respectivly. These must also be normalized as

$$\int_0^\infty \mathrm{d}r\,|u_0|^2 + \int_0^\infty \mathrm{d}r\,|u_2|^2 = 1, \tag{A.16}$$

and the two terms can be interpreted as a weight for the respective wave. Now using the expression for the deuteron wave function equation (A.15)

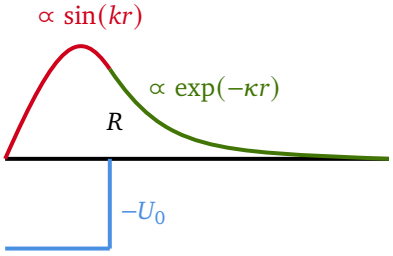

Figure A.2: The s-wave wave function for the deuteron.

	0^+	0^-	1^+	1^-
Singlet	$^1s_0$			$^1p_1$
Triplet		3_0^p	$^3s_1, ^3d_1$	$^3p_1$

Table A.1: Two nucleon states J^Π. The deuteron consists of a wave function superposition of $^3s_1 + ^3d_1$.

I want to get an expression for the differential cross section for the nuclear photoeffect. When an absorbed photon frequency is greater than the lowest threshold of nuclear decay the nucleus becomes excited to the continuum states. These states can decay in a number of ways but here are consider the case where the decay happens through particle emission. In other words this is the absorbtion of a photon that results in a particle decay into the continuum. From conservation of energy we have

$$E_i = \hbar\omega = E_f + \epsilon, \tag{A.17}$$

where the nucleus A goes from the inital state with energy E_i to the final state with $A-1$ and energy E_f and the particle in the continuum has energy $\epsilon = \mathbf{p}^2/2m$.

In contrast to the excitation of the discrete states that shows resonance behavior the continuum of energy states makes for a more smooth dependence. This means we can use what we know form the discrete excitation but introduce a level density ρ_f instead of the usual delta function in the expression for the differential cross section. This yields

$$\mathrm{d}\sigma_{fi} = \frac{4\pi^2\hbar}{E_\gamma c}\left|\sum_a \frac{\mathbf{e_a}}{m_a}\left\langle f\right|(\mathbf{p}_a\cdot\mathbf{e}_{\mathbf{k}\lambda})\mathrm{e}^{i(\mathbf{k}\cdot\mathbf{r}_a)}\left|i\right\rangle\right|^2 \rho_f, \tag{A.18}$$

where the level density is given by

$$\rho_f = \frac{Vmp}{(2\pi\hbar)^3}\mathrm{d}o. \tag{A.19}$$

Here the particle is emitted with momentum $\mathbf{p}$ into the solid angle element do and E_γ is the energy of the photon. In the case of the deuteron equation (A.18) and be split into different multipolarities and the most simple is the electric dipole transition ($E1$) from the deuteron bound state into the state of continuum motion of the proton and the neutron with reduced mass $m/2$.

In the long wave length limit the plane wave expression reduces to unity which means equation (A.18) for the dipole transition can be written as

$$\mathrm{d}\sigma_{E1} = \frac{\alpha mp\omega}{\hbar^2}\left|\sum_a(\mathbf{e}\cdot\mathbf{r_a})_{fi}\right|^2 \frac{\mathrm{d}o}{4\pi}, \tag{A.20}$$

where the solid angle could be the direction along the motion of the proton[1].

1. Also, $V=1$ and $\alpha = e^2/\hbar c$

When assuming an unpolarized deuteron we can take the average over the spin states $1/3\sum_m$ and count all final polarizations $\sum_{m'}$[2]. The final state is still spin triplet since the dipole operator does not act on the spin variable. This yields

2. Note m and m'

$$\overline{\mathrm{d}\sigma_{E1}} = \frac{1}{4}\frac{\alpha mp\omega}{\hbar^2}\frac{1}{3}\sum_{mm'}\left|(\mathbf{e}\cdot\mathbf{r})_{fi}\right|^2\frac{\mathrm{d}o}{4\pi}. \tag{A.21}$$

The task in now to find an expression for the dot product in the sum. The final spin state after the $E1$ transition remains a triplet with $S=J=1$, the orbital and parity, however, is not the same. The final state corresponds to the p-wave where the low-energy nuclear forces are weak and the wavelength of the relative motion is much larger than the range of those forces. From conservation of energy we have have

$$\frac{\hbar^2k^2}{2m} = \hbar\omega - \epsilon, \tag{A.22}$$

where ϵ is the binding energy of the deuteron also in equation (A.2). For any direction of the relative momentum vector $\hbar\mathbf{k}$ the p-wave component must be normalized through some Legendre polynomial $P_1(\cos(\theta))$ and the spherical Bessel function $j_{\ell=1}(kr)$.[3]

3. $P_1(\cos(\theta)) = \cos(\theta)$ and $j_1(\rho) = \frac{\sin(\rho)-\rho\cos(\rho)}{\rho^2}$.

Here θ is the angle between the relative coordinate $\mathbf{r}$ and the wave vector $\mathbf{k}$ this yields

$$\psi_f(r,\theta) = 3i\cos(\theta)j_1(kr)\chi_{mm'} \tag{A.23}$$

In the s-wave transition we get the following expression when integration over the angles of the unit vector $\mathbf{n} = \mathbf{r}/r$

$$\frac{1}{2}\left\langle f; m'\middle|(\mathbf{e}\cdot\mathbf{r})\middle|\ell = 0; m\right\rangle = -i\frac{\sqrt{\pi}}{k}(\mathbf{e}\cdot\mathbf{k})I_0\delta_{mm'}. \tag{A.24}$$

The radial integrals for the s-wave and d-wave are given by I_0 and I_2 respectively.[4] For the d-wave we have to reintroduce the tensor operator[5] S_12. Just like in the s-wave case we have to integrate over the unit vector – this time, however, it contains four components

4. $I_\ell = \int_0^\infty \mathrm{d}r\, r^2 j_1(kr)u_\ell(r)$, $\ell = 0, 2$

5.

$$S_{12}(\mathbf{n}) = 3(\boldsymbol{\sigma}_1\cdot\mathbf{n})(\boldsymbol{\sigma}_2)\cdot\mathbf{n} - (\boldsymbol{\sigma}_1\cdot\boldsymbol{\sigma}_2) = 2[3(\mathbf{S}\cdot\mathbf{n})^2 - \mathbf{S}^2]$$

$$\int \mathrm{d}o\, n_i n_j n_k n_l = \frac{4\pi}{15}(\delta ij\delta_{kl} + \delta_{ik}\delta_{jl} + \delta_{il}\delta_{jk}), \tag{A.25}$$

and the d-wave contribution is given by

$$\frac{1}{2}\left\langle f; m'\middle|(\mathbf{e}\cdot\mathbf{r})\middle|\ell = 2; m\right\rangle = -i\frac{\sqrt{\pi}}{k}C_{m'm}I_2, \tag{A.26}$$

where the spin matrix element $C_{mm'}$ contains

$$C = \frac{2\sqrt{2}}{5}\left[\frac{3}{4}\left[(\mathbf{k}\cdot\mathbf{S})(\mathbf{e}\cdot\mathbf{S}) + (\mathbf{e}\cdot\mathbf{S})(\mathbf{k}\cdot\mathbf{S})\right] - (\mathbf{e}\cdot\mathbf{k})\right]. \tag{A.27}$$

6.

$$\sum_{mm'}|O_{m'm}|^2 = \sum_m (O^\dagger O)_{mm} = \mathrm{Tr}\{O^\dagger O\}$$

Equation (A.27) can be rewritten using a trace identity[6] Skipping the calculation and moving back to equation (A.21) we have

$$\frac{1}{3}\sum_{mm'}\left|(\mathbf{e}\cdot\mathbf{r})_{fi}\right|^2 = 4\pi\left(I_0^2\cos^2(\alpha) + \frac{1}{25}I_2^2(3+\cos^2(\alpha))\right), \tag{A.28}$$

where α is the angle between $\mathbf{e}$ and the momentum of the final nucleon $\mathbf{k}$. The final steps involve averaging over the transverse polarizations of the initial photon which also relates the angle α to the experimentally observed angle between the directions of the photon and final nucleus. This means we get the following expression

$$\overline{\cos^2(\alpha)} = \frac{1}{2}\sin^2(\theta) \tag{A.29}$$

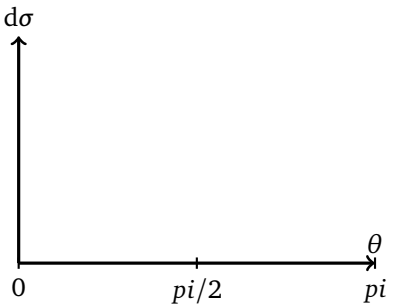

Figure A.3: Behavior of the differential cross section from equation (A.30).

Plugging this into equation (A.20) yields

$$\mathrm{d}\sigma_{E1} = \frac{\pi}{2}\frac{\alpha mp\omega}{\hbar^2}\left[I_0^2\sin^2(\theta) + \frac{1}{25}(6+\sin^2(\theta))I_2^2\right]\frac{\mathrm{d}o}{4\pi}, \tag{A.30}$$

and we arrive at the final expression when integrating over the angle of emitted photons

$$\sigma_{E1} = \frac{\pi}{3}\frac{\alpha mp\omega}{\hbar^2}\left(I_0^2 + \frac{2}{5}I_2^2\right). \tag{A.31}$$

If is also possible to estimate the cross section in equation (A.31) using the initial wave function of the approximation of weak binding. Here the wave function is replaced by its exponential tail outside the range of

nuclear forces. Furthermore, the contribution I_2 is neglected. This means the wave function is given by

$$\psi_i = \sqrt{\frac{\kappa}{2\pi}} \frac{e^{-\kappa r}}{r}, \tag{A.32}$$

where κ is defined in equation (A.5). Calculating the integral I_0 yields

$$\sigma = \frac{8\pi}{3} \frac{\alpha\hbar^2}{M} \frac{\sqrt{\epsilon}(\hbar\omega - \epsilon)^{3/2}}{(\hbar\omega)^3}, \tag{A.33}$$

which is rewritten in terms of the photon energy, $\xi = \hbar\omega/\epsilon$ and in terms of numerical estimates

$$\sigma(\xi) \simeq 1.2 \frac{(\xi - 1)^{3/2}}{\xi^3} \times 10^{-26}\,\mathrm{cm}^2. \tag{A.34}$$

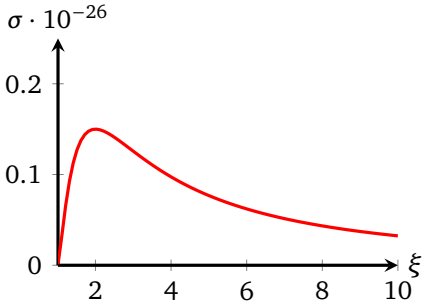

Figure A.4: Behavior of the cross section as a function of photon energy, ξ. Maximum occurs at $0.15 \cdot 10^{-26}$ cm^2 which is equivalent to 1.5 mb.

Appendix **B**

Special functions and properties

This appendix covers the basics of some of the special functions that arise when discussing the properties of some operators in quantum mechanics and formulae used.

B.1 Legendre polynomials and spherical Bessel functions

$$Y_\ell^m(\theta,\phi) = \frac{(-1)^{\ell l+m}}{(2\ell)!!}\left[\frac{(2\ell+1)(\ell-m)}{4\pi(\ell+m)!}\right](\sin\theta)^m \frac{\mathrm{d}^{\ell+m}}{(d\cos\theta)^{\ell+m}}[(\sin\theta)^{2\ell}]\exp\{im\phi\}, \tag{B.1}$$

which satisfy

$$Y_\ell^{*m} = (-1)^m Y_l^{-m}. \tag{B.2}$$

The spherical harmonics are connected to the Legendre polynomials

$$P_\ell(\cos\theta) = \left[\frac{4\pi}{2\ell+1}\right]^{1/2} Y_l^0(\theta). \tag{B.3}$$

Another important feature of spherical harmonics is that they form a complete set of functions over the unit sphere. Furthermore, they form an orthonormal set

$$\int \mathrm{d}\Omega\, Y_\ell^{*m} Y_{l'}^{m'} = \delta_{mm'}\delta_{ll'}. \tag{B.4}$$

Also, there exists an addition theorem for spherical harmonics

$$\sum_{m=-\ell} Y_\ell^{*m}(\theta,\phi) Y_\ell^m(\theta'.\phi') = \left(\frac{2\ell+1}{4\pi}\right)^{1/2} Y_\ell^0(\alpha) \tag{B.5}$$

The wave function of a plane wave with wave number k propagating along the z axis can be described by

$$\mathrm{e}^{ikz} = \mathrm{e}^{ikr\cos(\theta)} \tag{B.6}$$

$$= \sum_{\ell=0}^{\infty} A_\ell(r) Y_{\ell,0}(\theta), \tag{B.7}$$

where

$$A_\ell(r) = \int \mathrm{d}\Omega\, Y_{\ell,0}^*(\theta)\mathrm{e}^{ikr\cos(\theta)} = i^\ell\sqrt{4\pi(2\ell+1)}\, j_\ell(kr), \tag{B.8}$$

where the last equality shows the coefficient $A_\ell(r)$ can be expressed in terms of a spherical Bessel function $j_\ell(kr)$. Using the addition theorem

equation (B.6) yields the decomposition of a plane wave into spherical Bessel functions

$$e^{i\mathbf{k}\cdot\mathbf{r}} = 4\pi \sum_{\ell,m} i^\ell j_\ell(kr) Y_\ell^{m*}(\theta,\phi) Y_\ell^m(\theta,\phi) \tag{B.9}$$

B.2 Hankel transform

B.3 Coulomb wave functions

The Coulomb wave function for a charged particle with arbitrary angular momentum and charge is given by

$$\nabla^2\psi + \left(k^2 - \frac{2\mu}{\hbar^2}V(r)\right)\psi = 0, \tag{B.10}$$

where μ is the reduced mass of the system. The radial wave function $u(r)$ satisfied the following differential equation

$$\frac{\mathrm{d}^2 u\ell}{\mathrm{d}r^2} + \left(k^2 - \frac{\ell(\ell+1)}{r^2} - \frac{2\mu}{\hbar^2}\frac{Ze^2}{r}\right), \tag{B.11}$$

where Z is the product of the charges. Two independent solutions can be found to equation (B.11)–these are called the regular and irregular Coulomb wave functions denoted $F_\ell(r)$ and $G_\ell(r)$ respectively. The regular Coulomb wave function $F_\ell(r)$ is a real function that vanishes at $r = 0$ and the behaviour of the function is described using a parameter η which describes how strongly the Coulomb interaction is

$$\eta = \frac{Zmc\alpha}{\hbar k}, \tag{B.12}$$

where m is the mass of the particle, k is the wave number and α is the fine structure constant. The solution to is given by

$$F_\ell(\eta, kr) = C_\ell(\eta)(kr)^{\ell+1} e^{-ikr} {}_1F_1(\ell+1-i\eta, 2\ell+2, 2ikr), \tag{B.13}$$

where ${}_1F_1(kr)$ is a confluent hypergeometric function and $C_\ell(\eta)$ is a normalization constant given by

$$C_\ell(\eta) = \frac{2^\ell e^{-\pi\eta/2}\left|\Gamma(\ell+1+i\eta)\right|}{(2\ell+1)!}, \tag{B.14}$$

where Γ is the gamma function. For numerical purposes, it is useful to use the integral representation of equation (B.13) [**NIST**]

$$F_\ell(\eta,\rho) = \frac{\rho^{\ell+1}2^\ell e^{i\rho-(\pi\eta/2)}}{|\Gamma(\ell+1+i\eta)|}\int_0^1 e^{-2i\rho t} t^{\ell+i\eta}(1-t)^{\ell-i\eta}\,\mathrm{d}t. \tag{B.15}$$

For particles without charge, we can ignore the Coulomb interaction in equation (B.11) and the solution becomes

$$F_\ell(\eta,\rho) = \left(\frac{\pi kr}{2}\right)^{1/2} J_{\ell+1/2}(kr), \quad \text{particles without charge} \tag{B.16}$$

where $J_{\ell+1/2}$ is a Bessel function. Equation (B.16) is nothing but a spherical Bessel function. This means in the limit where the particles become chargeless the solution must reduce to a plane wave solution.

Appendix C

Three component wavefunction

Strictly speaking, the nuclear model should be consistent with other results from nuclear physics. In particular, the mass difference between the charged pion and the neutral pion. A priori we do not know the impact on the wave function of the nucleon-pion system and in this appendix, we wish to estimate how the wave function changes when we take the different properties of the pion into account. Starting from (**??**)

$$\psi_p = p\uparrow\frac{1}{\sqrt{V}}, \quad \psi_{N\pi^0} = (\boldsymbol{\tau}\cdot\boldsymbol{\pi})(\boldsymbol{\sigma}\cdot\mathbf{r})\phi_0(r)p\uparrow\frac{1}{\sqrt{V}}, \quad \psi_{N\pi^+} = (\boldsymbol{\tau}\cdot\boldsymbol{\pi})(\boldsymbol{\sigma}\cdot\mathbf{r})\phi_+(r)p\uparrow\frac{1}{\sqrt{V}}, \tag{C.1}$$

and these will act as the state vector in our system. Constructing a similar Hamiltonian for the three-component wave function yields

$$\begin{bmatrix} K_{\mathbf{p}} & W^\dagger & W^\dagger \\ W & K_{\mathbf{p}} + K_0 + m_{\pi^0} & 0 \\ W & 0 & K_{\mathbf{p}} + K_+ + m_{\pi^+} \end{bmatrix} \begin{bmatrix} \psi_p \\ \psi_{N\pi^0} \\ \psi_{N\pi^+} \end{bmatrix} = E \begin{bmatrix} \psi_p \\ \psi_{N\pi^0} \\ \psi_{N\pi^+} \end{bmatrix}, \tag{C.2}$$

where K_i is the kinetic operator and W, $W^\dagger$ are the creation and annihilation of a pion respectively. This leads to three coupled equations

$$W^\dagger\psi_{N\pi^0} + W^\dagger\psi_{N\pi^+} = E\psi_p \tag{C.3}$$
$$W\psi_p + (K_0 + m_{\pi^0})\psi_{N\pi^0} = E\psi_{N\pi^0} \tag{C.4}$$
$$W\psi_p + (K_+ + m_{\pi^+})\psi_{N\pi^+} = E\psi_{N\pi^+}. \tag{C.5}$$

The calculations are completely analogous to what is done in chapter 3 and the final set of equations are given by

$$\left.\begin{aligned} &12\pi\int_0^\infty \mathrm{d}r\, f(r)\phi_0(r)r^4 + 12\pi\int_0^\infty \mathrm{d}r\, f(r)\phi_+(r)r^4 = E \\ &f(r) - \tfrac{\hbar^2}{2\mu_0}\left(\tfrac{\mathrm{d}^2\phi_0(r)}{\mathrm{d}r^2} + \tfrac{4}{r}\tfrac{\mathrm{d}\phi_0(r)}{\mathrm{d}r}\right) + m_\pi^0 c^2\phi_0(r) = E\phi_0(r) \\ &f(r) - \tfrac{\hbar^2}{2\mu_+}\left(\tfrac{\mathrm{d}^2\phi_+(r)}{\mathrm{d}r^2} + \tfrac{4}{r}\tfrac{\mathrm{d}\phi_+(r)}{\mathrm{d}r}\right) + m_\pi^+ c^2\phi_+(r) = E\phi_+(r) \end{aligned}\right\} \tag{C.6}$$

Physically, we have added another pion wave function to our original model yet it is still bound by the total energy of the system, E. Numerically this is almost the same system and the solutions can be found using the same numerical considerations as in section 3.4. The results are shown in C.1

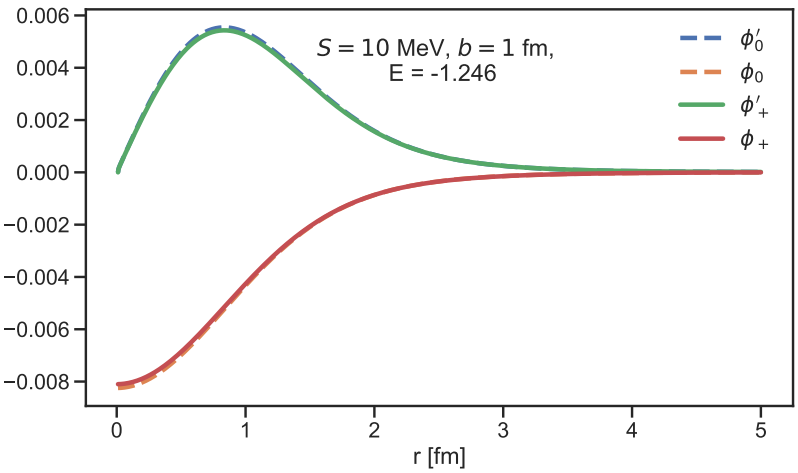

Figure C.1: Solutions to (C.6). The difference in the wave function is minimal compared to the two-component wave function. The energy is approximately equal to the sum of the two individual systems.

Compared to 3.4 the difference is negligible even accounting for the mass difference for the pions and nucleons (m_N, m_P). This means we can to a good estimation continue using only one pion wave function in our nuclear model.

Bibliography

[1] R. Beck et al. "Measurement of the p(γ,π^0) cross section at threshold". In: *Phys. Rev. Lett.* 65 (15 Oct. 1990), pp. 1841–1844. DOI: 10.1103/PhysRevLett.65.1841. URL: https://link.aps.org/doi/10.1103/PhysRevLett.65.1841.

[2] D. V. Fedorov. "A Nuclear Model with Explicit Mesons". In: *Few-Body Systems* 61.4 (Oct. 2020). ISSN: 1432-5411. DOI: 10.1007/s00601-020-01573-1. URL: http://dx.doi.org/10.1007/s00601-020-01573-1.

[3] A. Schmidt et al. "Test of Low-Energy Theorems for ${}^1H(\vec{\gamma},\pi^0){}^1H$ in the Threshold Region". In: *Phys. Rev. Lett.* 87 (23 Nov. 2001), p. 232501. DOI: 10.1103/PhysRevLett.87.232501. URL: https://link.aps.org/doi/10.1103/PhysRevLett.87.232501.

[4] Vladimir Zelevinsky and Alexander Volya. *Physics of Atomic Nuclei*. First. Wiley-VCH, 2017.